Supplement of Clim. Past, 15, 521–537, 2019
https://doi.org/10.5194/cp-15-521-2019-supplement


Climate of the Past
Open Access
EGU

*Supplement of*

# Empirical estimate of the signal content of Holocene temperature proxy records

**Maria Reschke et al.**

*Correspondence to:* Maria Reschke (mreschke@awi.de)

**Supplementary Figures**

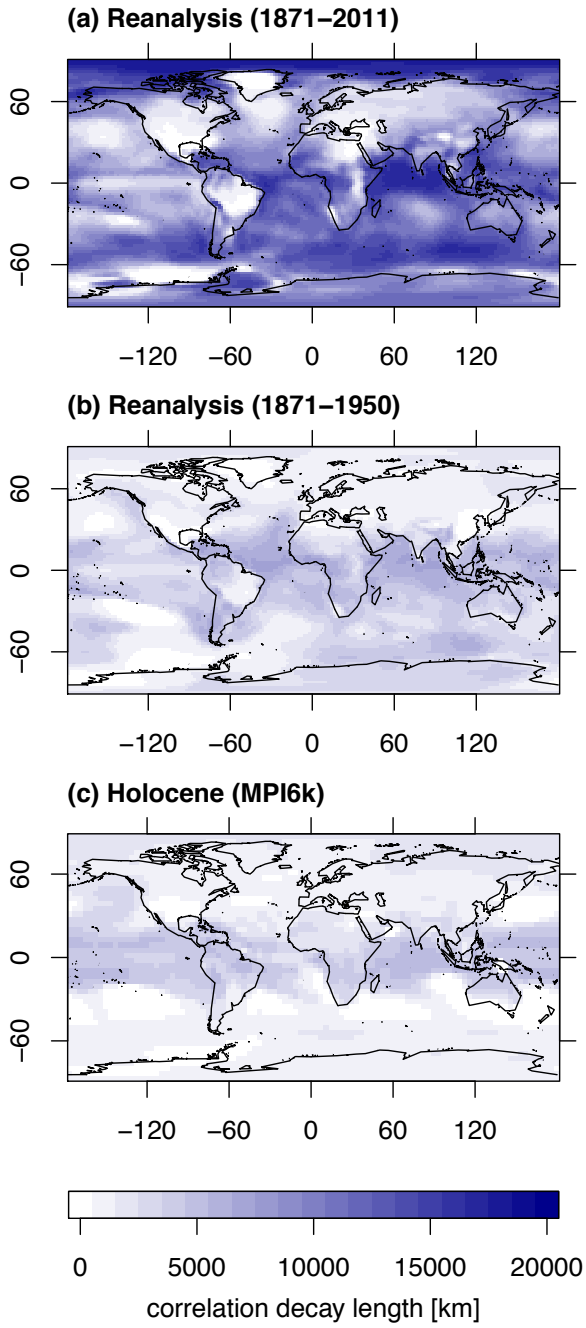


**Figure S1: Correlation decay length of annual mean surface temperature data from reanalysis data (Compo et al., 2006) and the MPI6k model simulation.** Due to an increased anthropogenic forcing, analysing the entire reanalysis data (a) results in a much higher correlation decay length than just analysing the time-period 1871 to 1950 (b). The similarity of the results of the reanalysis data from 1871 to 1950 and the Holocene model simulation data (c) indicates that the spatial correlation structure in MPI6k is reasonable.

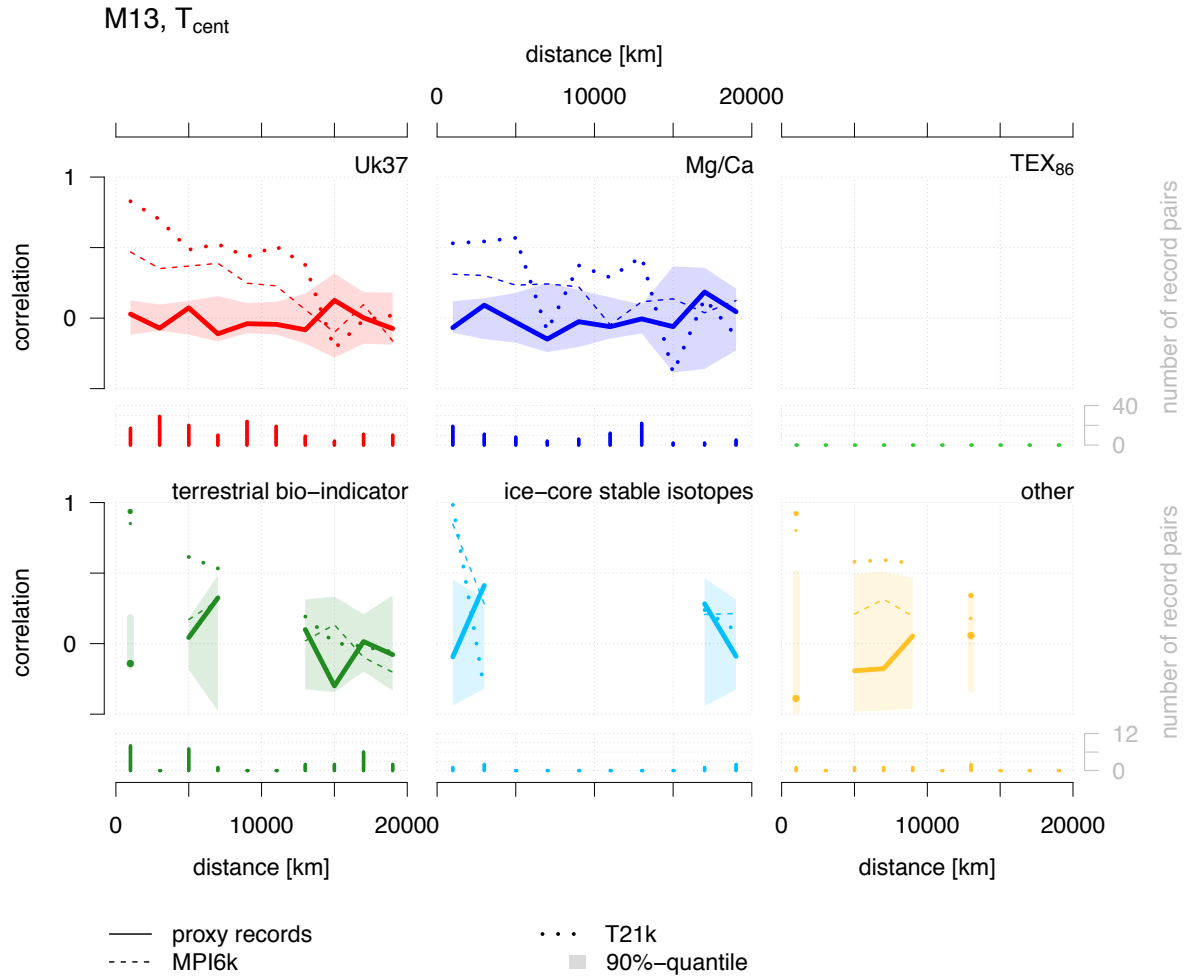


**Figure S2: Proxy-type-specific spatial correlation ($T_{cent}$) of Holocene temperature proxy records and simulated surface air temperatures based on the M13 dataset.** The upper parts of the panels show mean correlations of 2000 km sized bins as a function of the separation distance between record pairs in model time series at proxy positions (dotted/dashed line) and proxy records (continuous line). Coloured polygons represent the 90%-quantile of mean correlations of uncorrelated surrogate time series with a power-law scaling of $\beta = 1$. The lower parts of the panels show the number of record pairs used for each estimate. Independent of the proxy type the spatial correlation of proxy records is not statistically significant. In contrast, model time series show a high correlation for close sites.

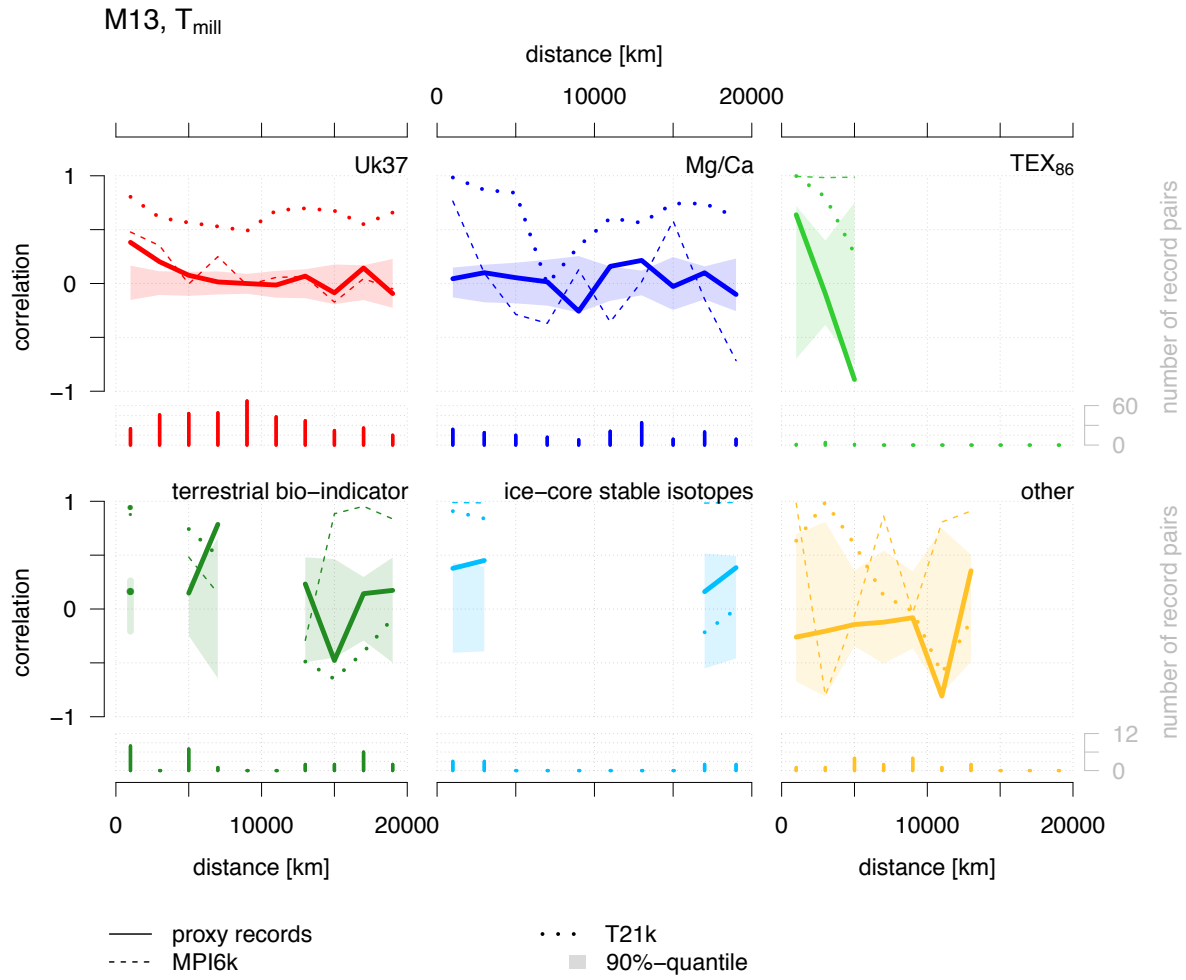


**Figure S3: Proxy-type-specific spatial correlation ($T_{mill}$) of Holocene temperature proxy records and simulated surface air temperatures based on the M13 dataset.** The upper parts of the panels show mean correlations of 2000 km sized bins as a function of the separation distance between proxy record pairs (continuous line) and pairs of model time series extracted at proxy positions (dotted/dashed line). Coloured polygons show the 90%-quantile of mean correlations of uncorrelated surrogate time series with a power-law scaling of $\beta = 1$. The lower parts of the panels illustrate the number of time series pairs used for each estimate. Underrepresented proxy types such as $TEX_{86}$, terrestrial bio-indicators, ice-core stable isotopes and others show statistically not significant spatial correlations of proxy records. Despite of a higher number of proxy time series, Mg/Ca-based estimates are not and Uk37-based ones are only statistically significant for close sites (separation <6000 km).

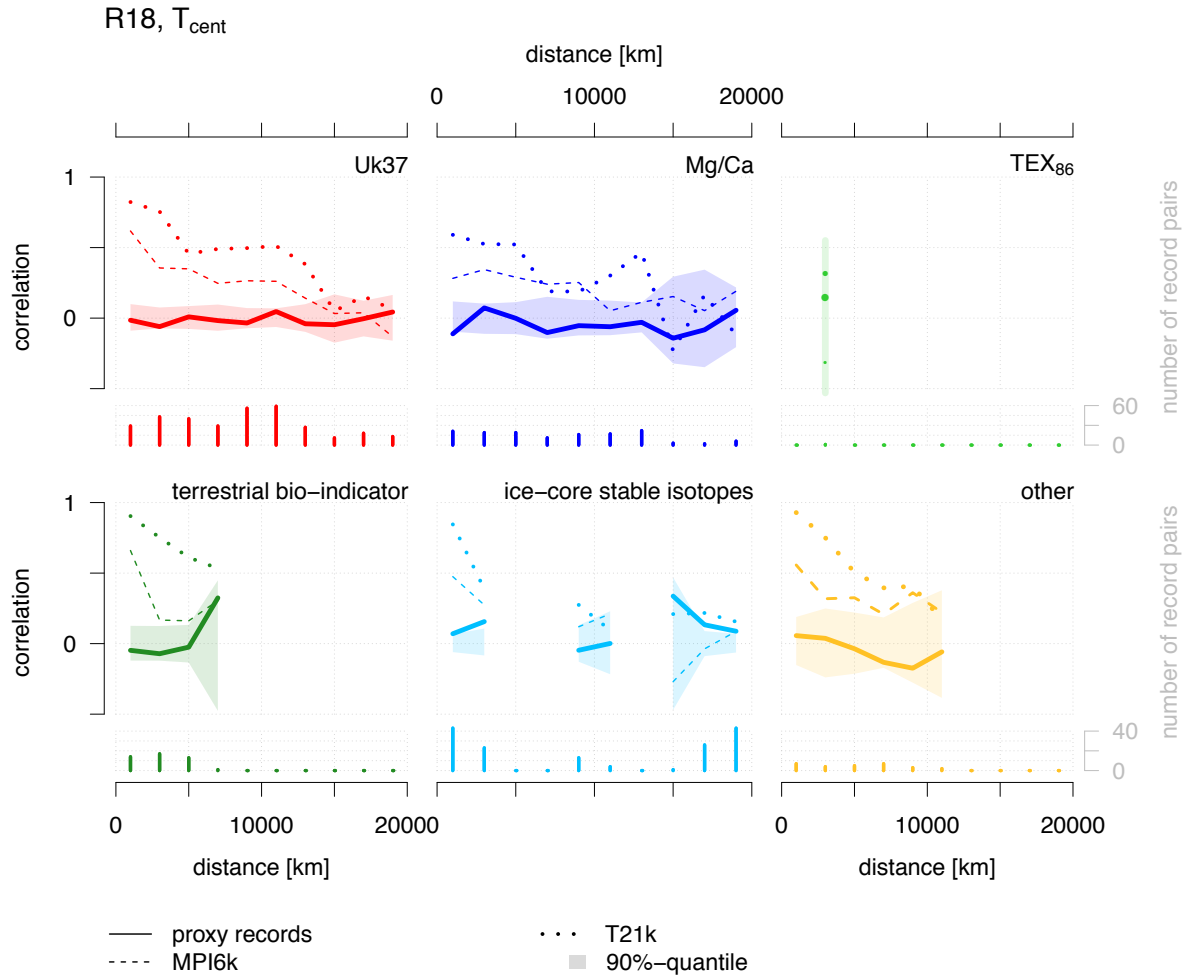


**Figure S4: Proxy-type-specific spatial correlation ($T_{cent}$) of Holocene temperature proxy records and simulated surface air temperatures based on the R18 dataset.** The upper parts of the panels illustrate mean correlations of 2000 km sized bins as a function of the separation distance between model time series at proxy positions (dotted/dashed line) and proxy datasets (continuous line). Coloured polygons mark the 90%-quantile of mean correlations of uncorrelated time series with a power-law scaling of $\beta = 1$. The lower parts of the panels show the number of record pairs used for each estimate. As in Figure S1, the proxy-type-specific spatial correlation based on proxy records is statistically not significant for all proxy types.

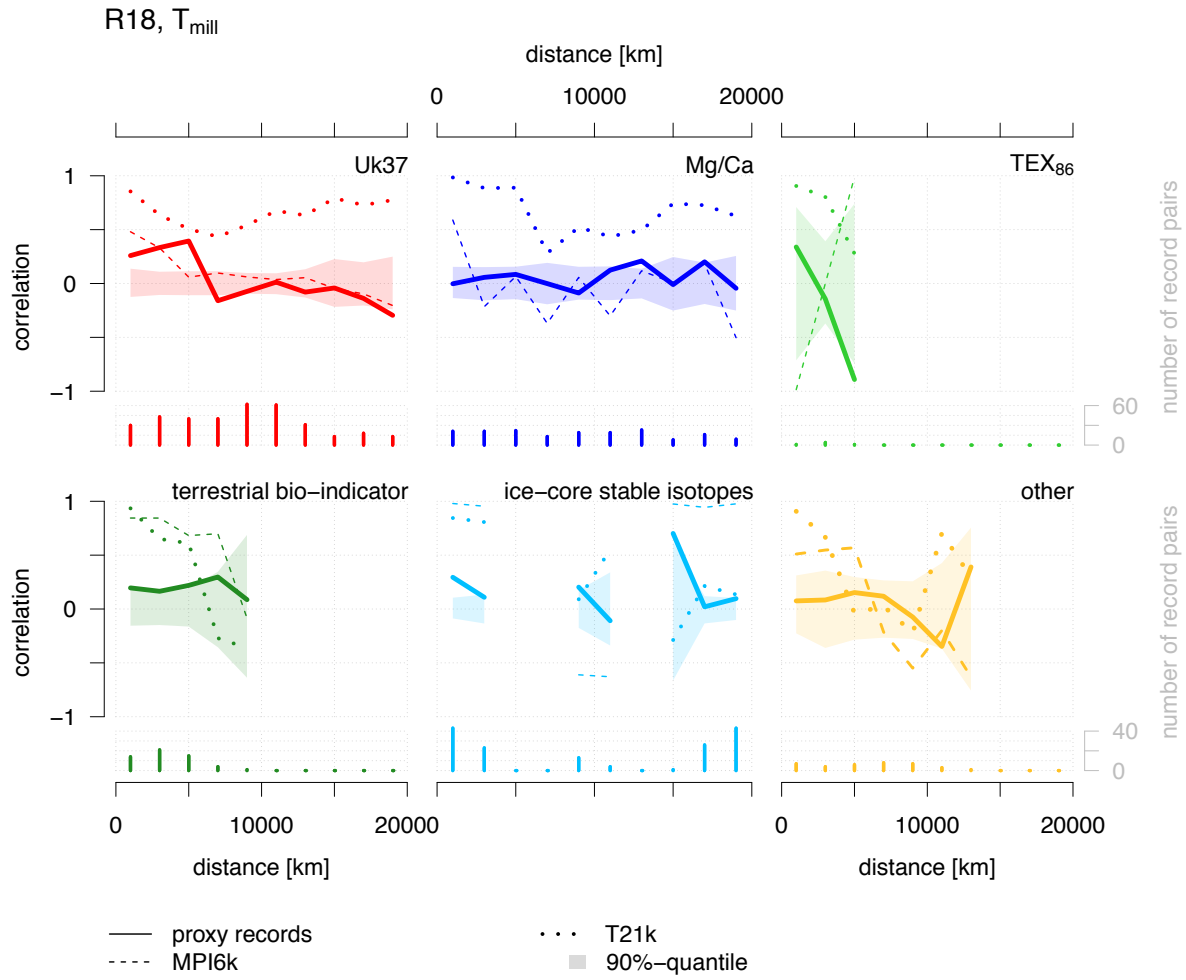


**Figure S5: Proxy-type-specific spatial correlation ($T_{mill}$) of Holocene temperature proxy records and simulated surface air temperatures based on the R18 dataset.** The upper parts of the panels depict mean correlations of 2000 km sized bins as a function of the separation distance between proxy (continuous line) and model time series extracted at proxy positions (dotted/dashed line). The coloured polygons mark the 90%-quantile of mean correlations of uncorrelated surrogate time series with a power-law scaling of $\beta = 1$. The lower parts of the panels show the number of record pairs used for each estimate. As in Figure S2, only Uk37-based time series are statistically significant for close sites (separation <6000 km).

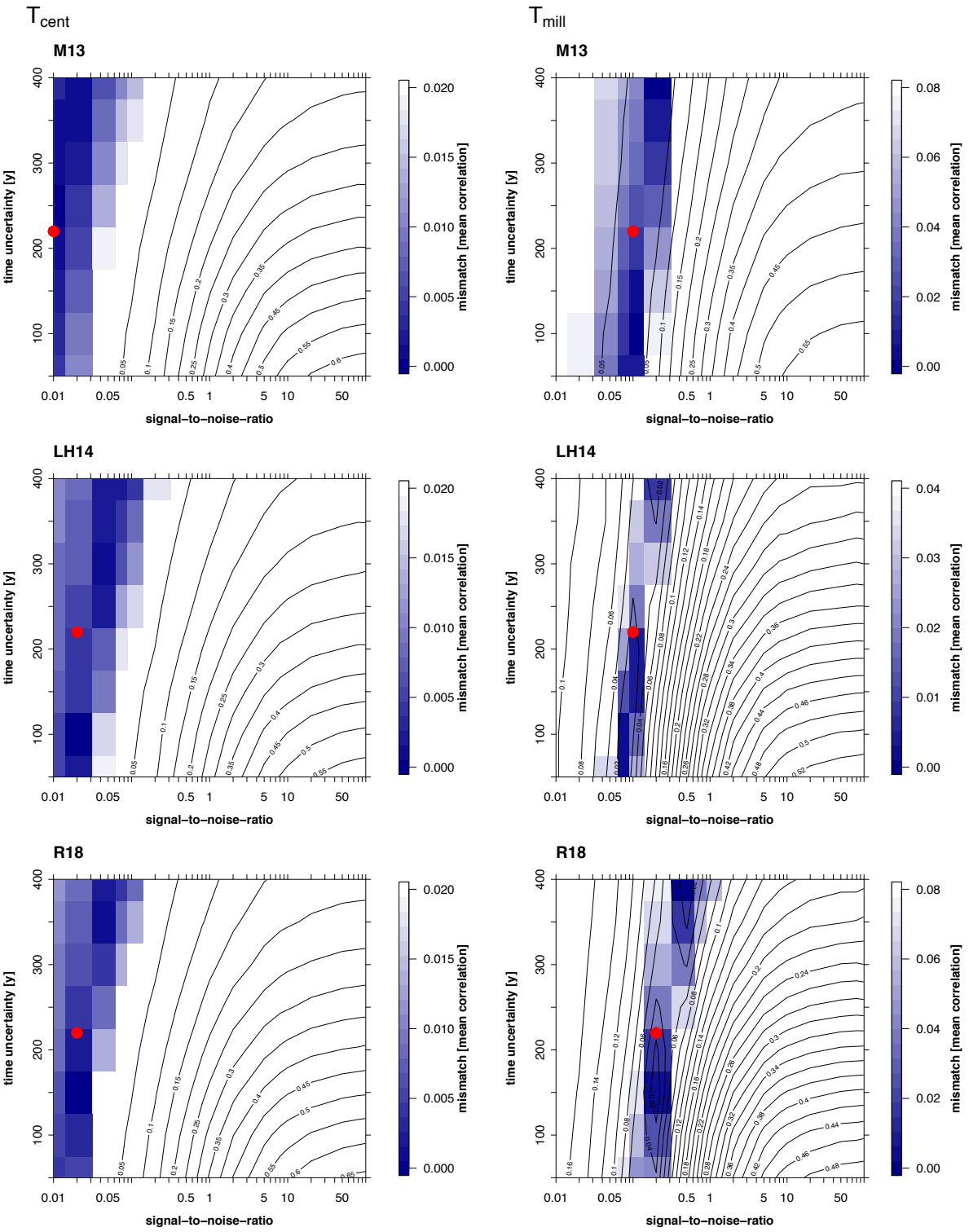


**Figure S6: $SNR_{T21k}$ estimates of Holocene temperature proxy records as a function of time uncertainty related to centennial $T_{cent}$ and centennial to millennial time scales $T_{mill}$.** Each panel shows the mismatch between mean correlations of close-by (separation <5000 km) proxy records and model time series extracted at proxy locations from model T21k (TraCE-21ka model simulation) as a function of time uncertainty (vertical axis) and SNR (horizontal axis). Parts with the same mismatch are illustrated by contour lines with numbers. Coloured areas belong to the lowest mismatch and show suitable combinations of $SNR_{T21k}$ estimates and time uncertainties. The SNRs are consistent for all datasets and show smaller estimates on $T_{cent}$ ($SNR_{T21k,T_{cent}} < 0.05$) than on $T_{mill}$ ($0.05 < SNR_{T21k,T_{mill}} < 0.2$). The red dots illustrate SNRs for a time uncertainty of 220y which is the mean provided uncertainty in M13.

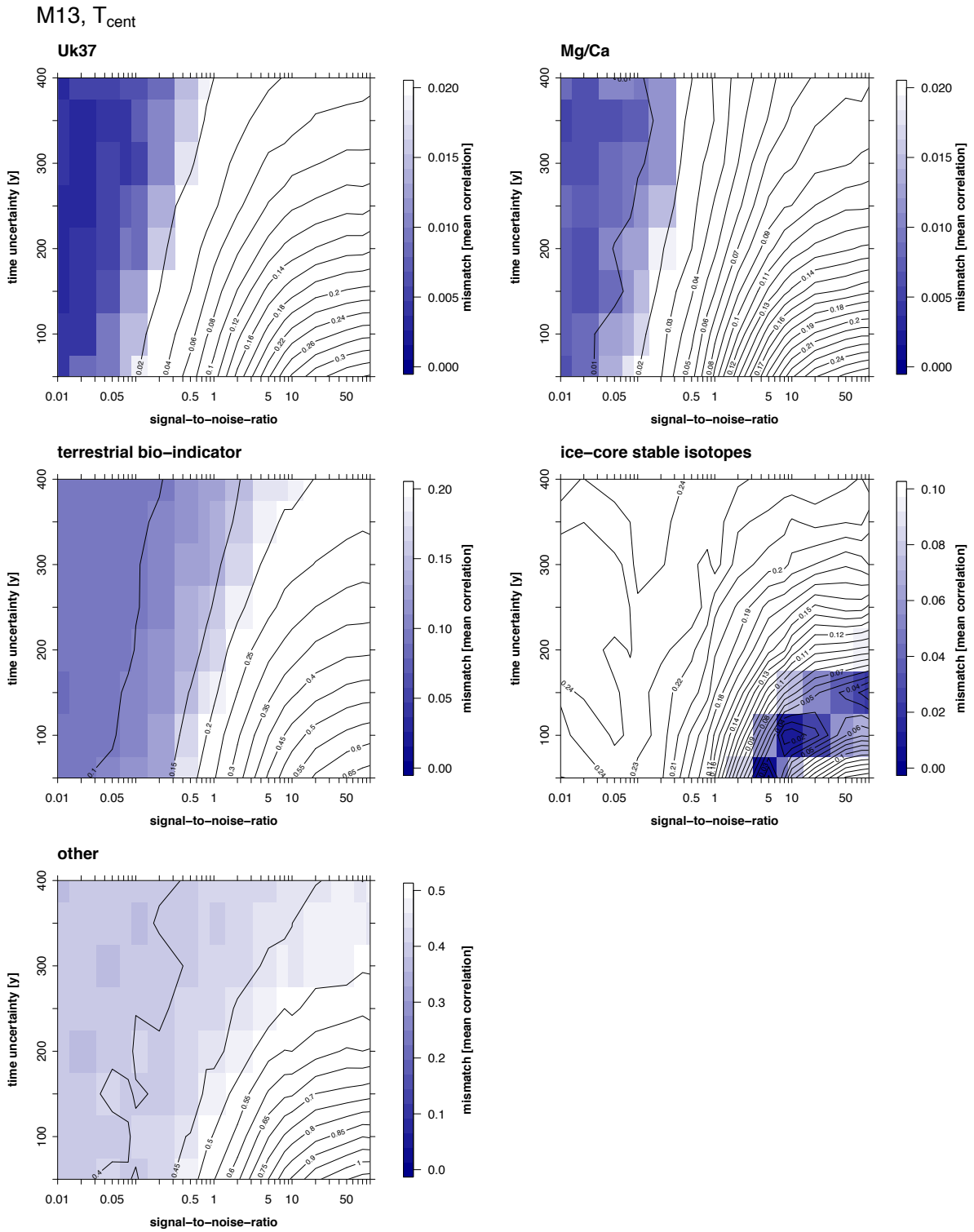


**Figure S7: Proxy-type-specific $SNR_{MPI6k,T_{cent}}$ estimates of Holocene temperature proxy records as a function of time uncertainty based on the M13 dataset and related to centennial time scales $T_{cent}$.** The panels show the mismatch between mean correlations of close-by (separation <5000 km) proxy records and model time series extracted at proxy locations from model MPI6k (ECHAM5/MPI-OM) as a function of time uncertainty (vertical axis) and SNR (horizontal axis). Contour lines with numbers illustrate areas with the same mismatch. Coloured parts of the panels mark suitable combinations of SNR estimates and time uncertainties (lowest mismatch). Except for ice-core stable isotopes, all proxy types are characterised by low $SNR_{MPI6k,T_{cent}}$ estimates on $T_{cent}$.

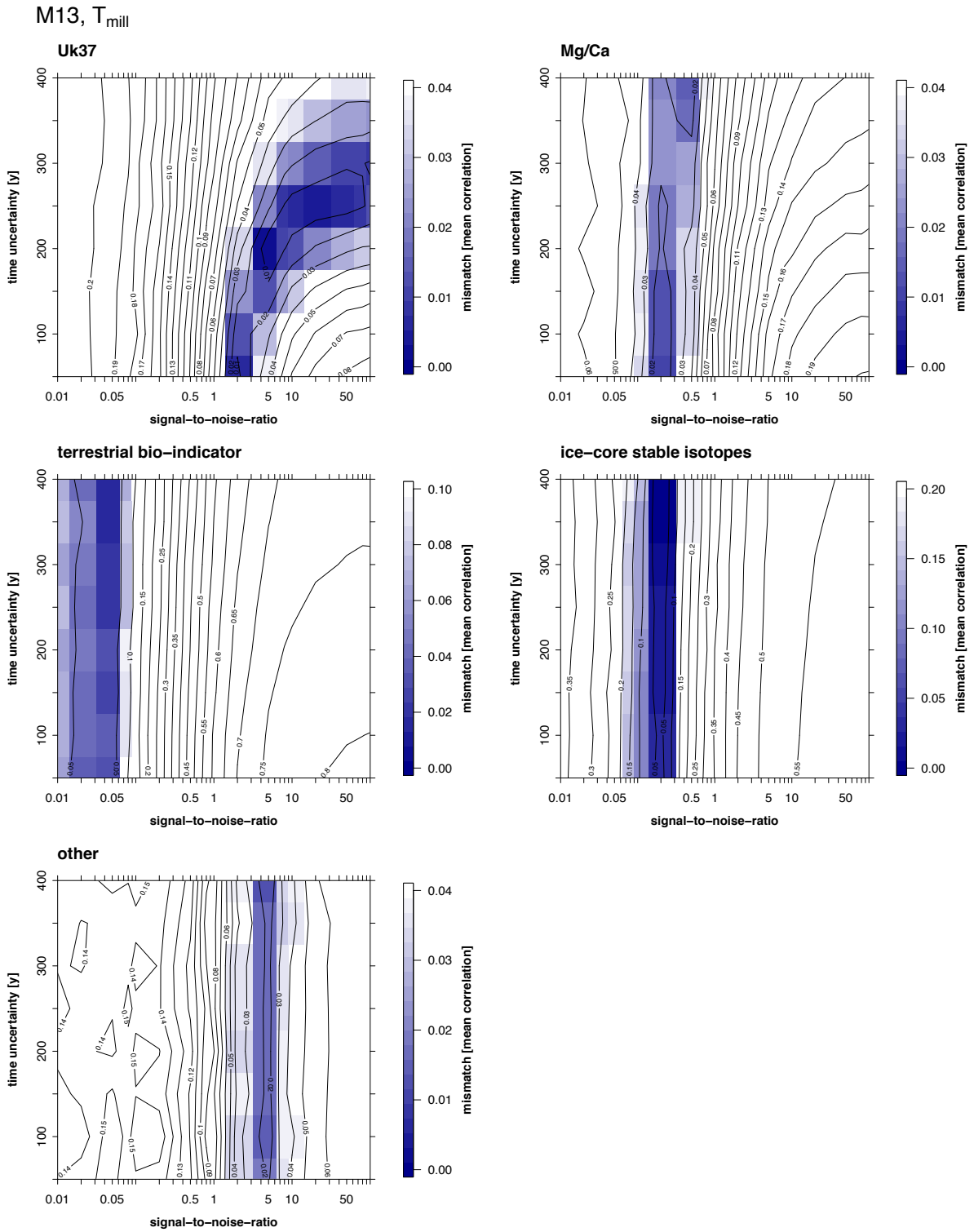


**Figure S8: Proxy-type-specific $SNR_{MPI6k,T_{mill}}$ estimates of Holocene temperature proxy records as a function of time uncertainty based on the M13 dataset and related to centennial to millennial time scales $T_{mill}$.** Each panel illustrates the mismatch between mean correlations of close-by (separation <5000 km) proxy records and model time series extracted at proxy locations from the model MPI6k (ECHAM5/MPI-OM) as a function of time uncertainty (vertical axis) and SNR (horizontal axis). Contour lines show parts with the same mismatch (numbers) and coloured areas (lowest mismatch) highlight suitable combinations of SNR estimates and time uncertainties. Most of the proxy-type-specific estimates indicate higher SNRs compared to $T_{cent}$. Except for Uk37, the estimated SNRs show a low dependence on time uncertainty.

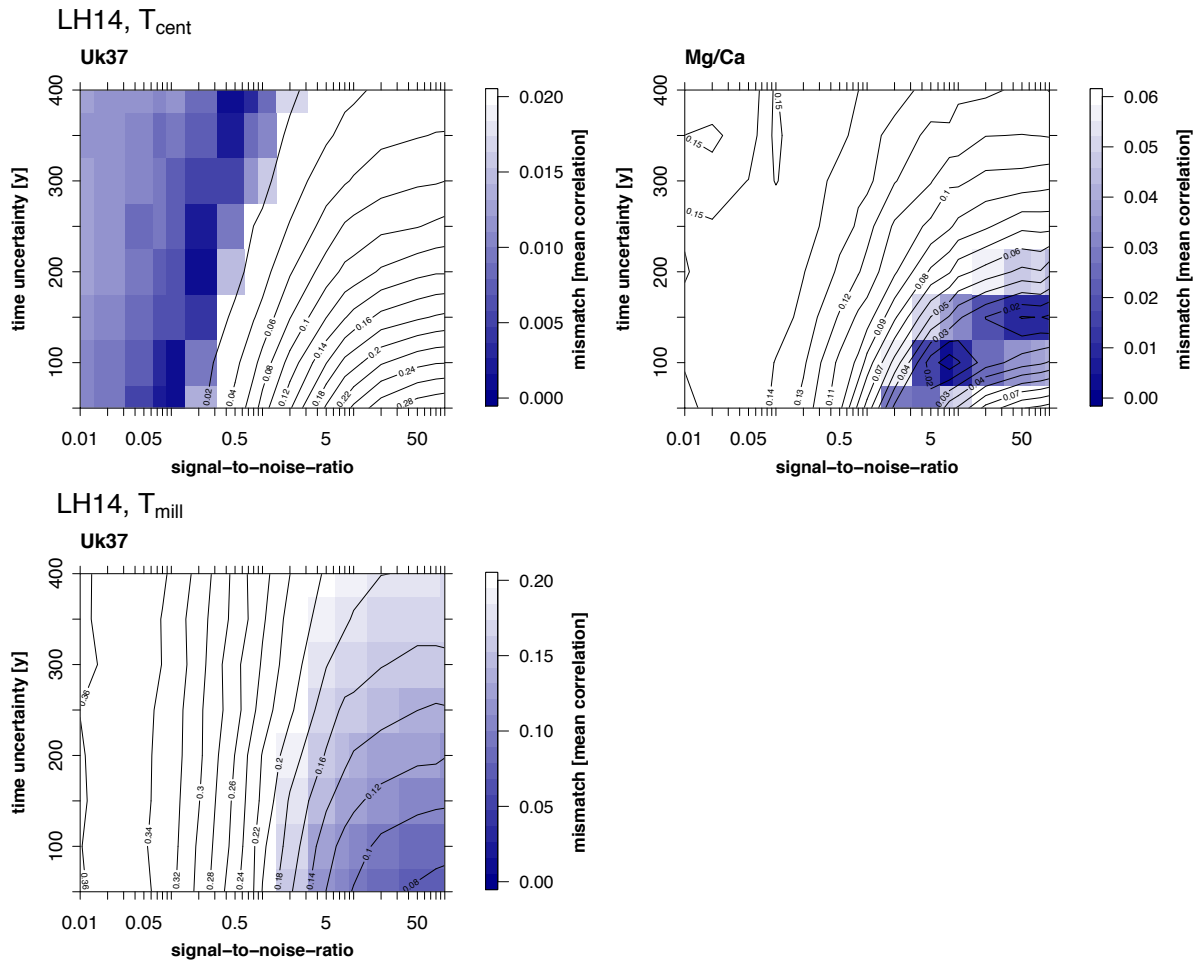


**Figure S9: Proxy-type-specific SNR estimates of Holocene temperature proxy records as a function of time uncertainty based on the LH14 dataset and related to centennial $T_{cent}$ and centennial to millennial time scales $T_{mill}$.** Panels show the mismatch between mean correlations of close-by (separation <5000 km) proxy records and model time series extracted from the model MPI6k (ECHAM5/MPI-OM) at proxy locations as a function of time uncertainty (vertical axis) and SNR (horizontal axis). Contour lines with numbers illustrate areas with the same mismatch. Coloured areas show the lowest mismatch and mark suitable combinations of SNR estimates and time uncertainties. On $T_{cent}$, Uk37-based estimates are low and Mg/Ca-based ones are high. $T_{mill}$ related SNR estimates for Mg/Ca are not possible as the mean correlations of the proxy time series are higher than the mean correlations of the model time series.

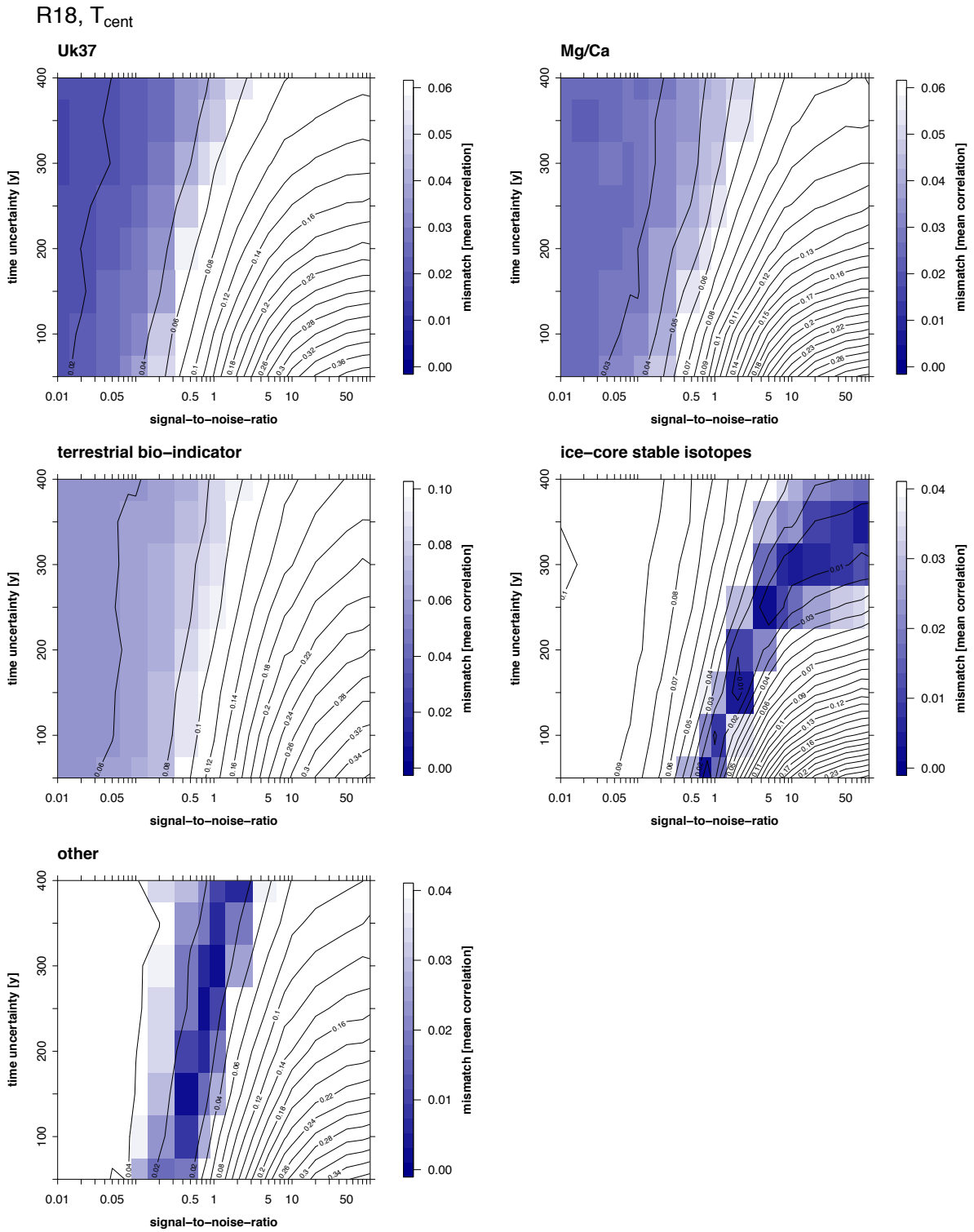


**Figure S10: Proxy-type-specific $SNR_{MPI6k,T_{cent}}$ estimates of Holocene temperature proxy records as a function of time uncertainty based on the R18 dataset and related to centennial time scales $T_{cent}$.** Each panel illustrates the mismatch between mean correlations of close-by (separation <5000 km) proxy records and model time series extracted at proxy locations from model MPI6k (ECHAM5/MPI-OM) as a function of time uncertainty (vertical axis) and SNR (horizontal axis). Contour lines with numbers mark parts with the same mismatch. Coloured areas highlight suitable combinations of SNR estimates and time uncertainties (lowest mismatch). Except for ice-core stable isotopes, all proxy types have estimated $SNR_{MPI6k,T_{cent}} < 1$.

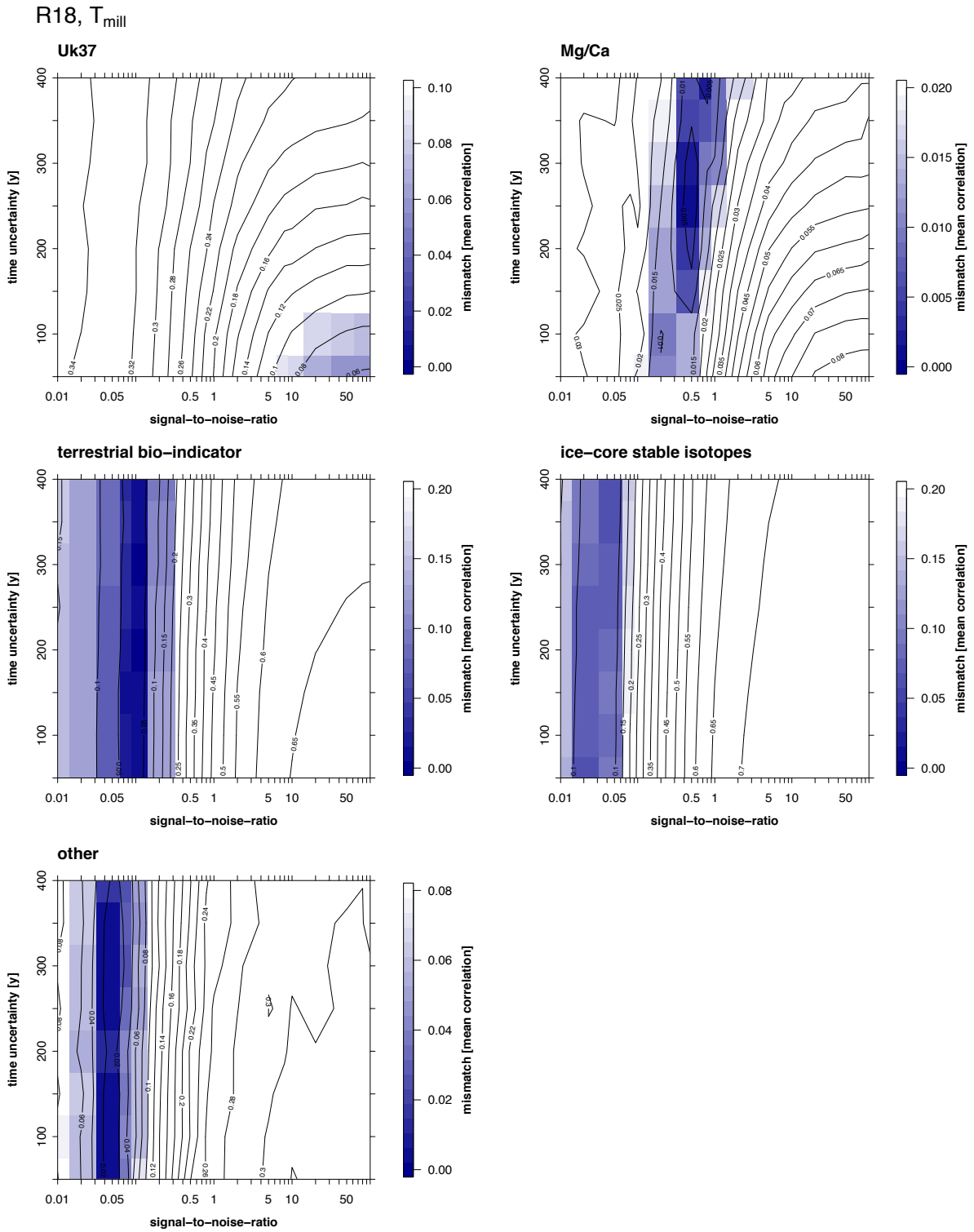


**Figure S11: Proxy-type-specific $SNR_{MPI6k,T_{mill}}$ estimates of Holocene temperature proxy records as a function of time uncertainty based on the R18 dataset and related to centennial to millennial time scales $T_{mill}$.** The panels show the mismatch between mean correlations of close-by (separation <5000 km) proxy records and model time series extracted at proxy locations from model MPI6k (ECHAM5/MPI-OM) as a function of time uncertainty (vertical axis) and SNR (horizontal axis). Contour lines mark parts with the same mismatch (numbers) and coloured areas (lowest mismatch) highlight suitable combinations of SNR estimates and time uncertainties. Most proxy-type-specific estimates indicate low SNRs. Very high SNR estimates are related to Uk37.

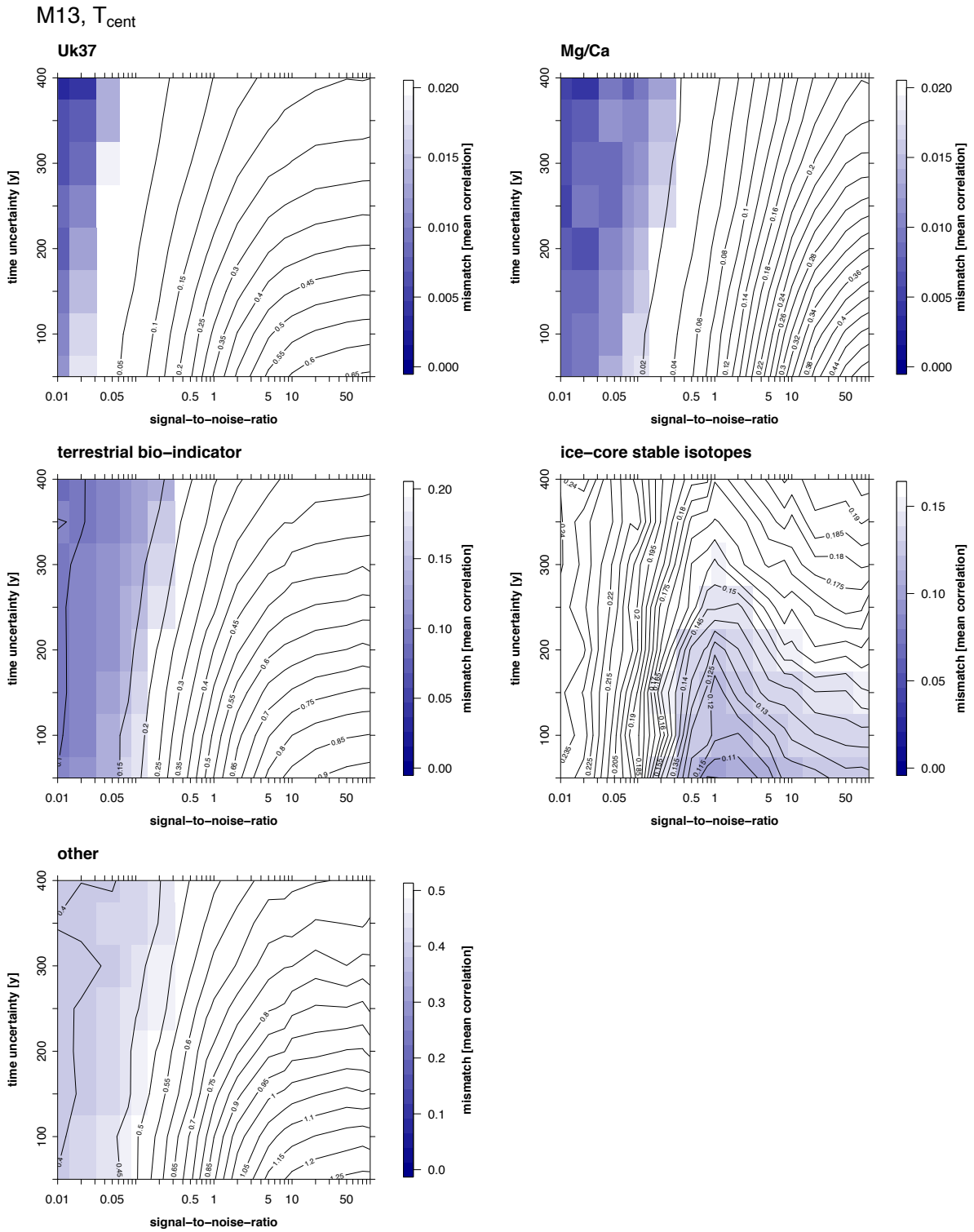


**Figure S12: Proxy-type-specific $SNR_{T21k,T_{cent}}$ estimates of Holocene temperature proxy records as a function of time uncertainty based on the M13 dataset and related to centennial time scales $T_{cent}$.** Each panel shows the mismatch between mean correlations of close-by (separation <5000 km) proxy records and model time series extracted at proxy locations from model T21k (TraCE-21ka model simulation) as a function of time uncertainty (vertical axis) and SNR (horizontal axis). Contour lines with numbers illustrate areas with the same mismatch. Coloured parts of the panels mark suitable combinations of SNR estimates and time uncertainties (lowest mismatch). Most proxy types are characterised by very low $SNR_{T21k,T_{cent}}$ estimates. Ice-core stable isotopes show high SNRs combined with lower time uncertainties.

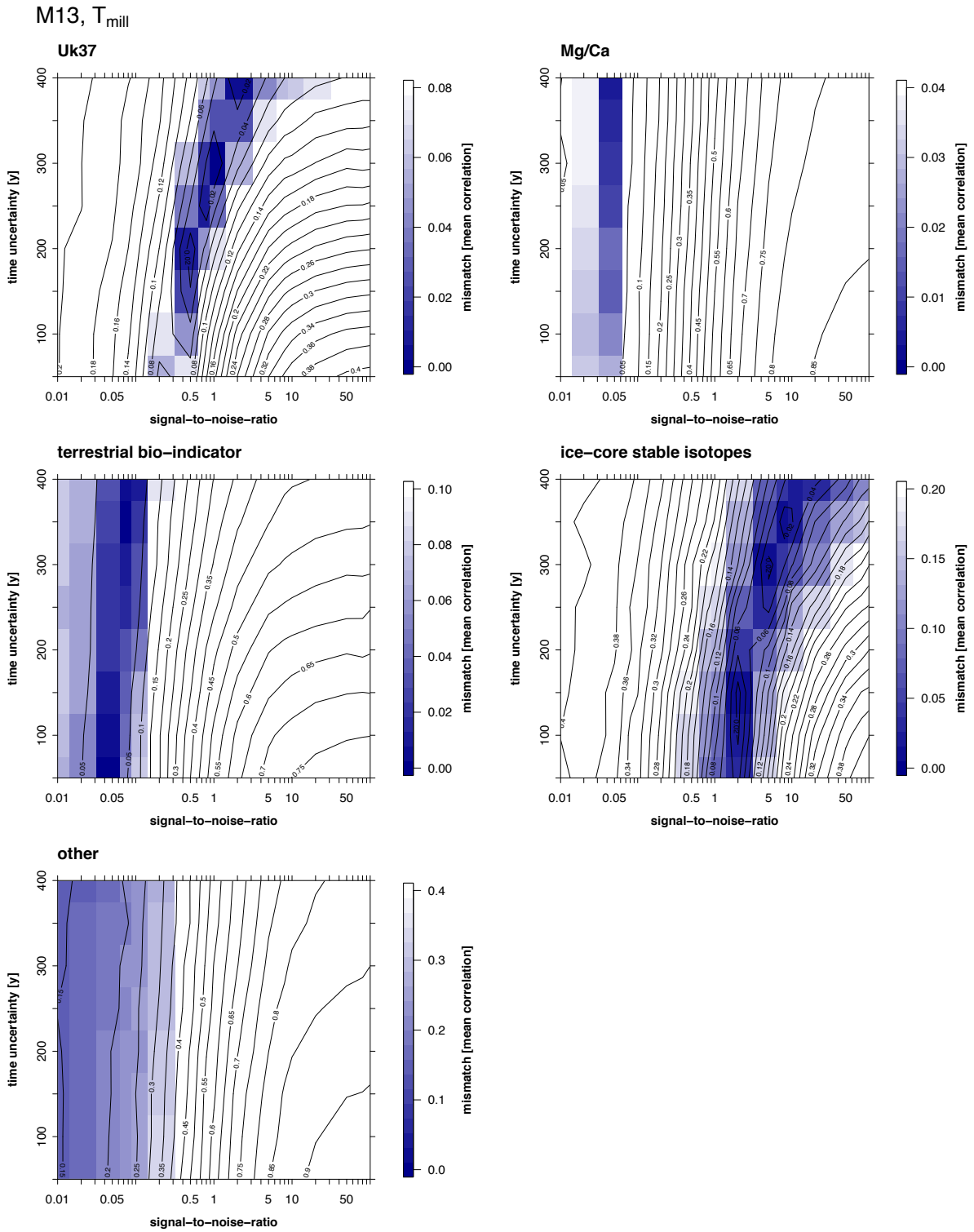


**Figure S13: Proxy-type-specific $SNR_{T21k,T_{mill}}$ estimates of Holocene temperature proxy records as a function of time uncertainty based on the M13 dataset and related to centennial to millennial time scales $T_{mill}$.** The panels illustrate the mismatch between mean correlations of close-by (separation <5000 km) proxy records and model time series extracted at proxy locations from model T21k (TraCE-21ka model simulation) as a function of time uncertainty (vertical axis) and SNR (horizontal axis). Contour lines show parts with the same mismatch (numbers) and coloured areas (lowest mismatch) highlight suitable combinations of SNR estimates and time uncertainties. All proxy-type-specific estimates indicate higher SNRs compared to $T_{cent}$. Except for Uk37 and ice-core stable isotopes, the estimated SNRs show a low dependence on time uncertainty.

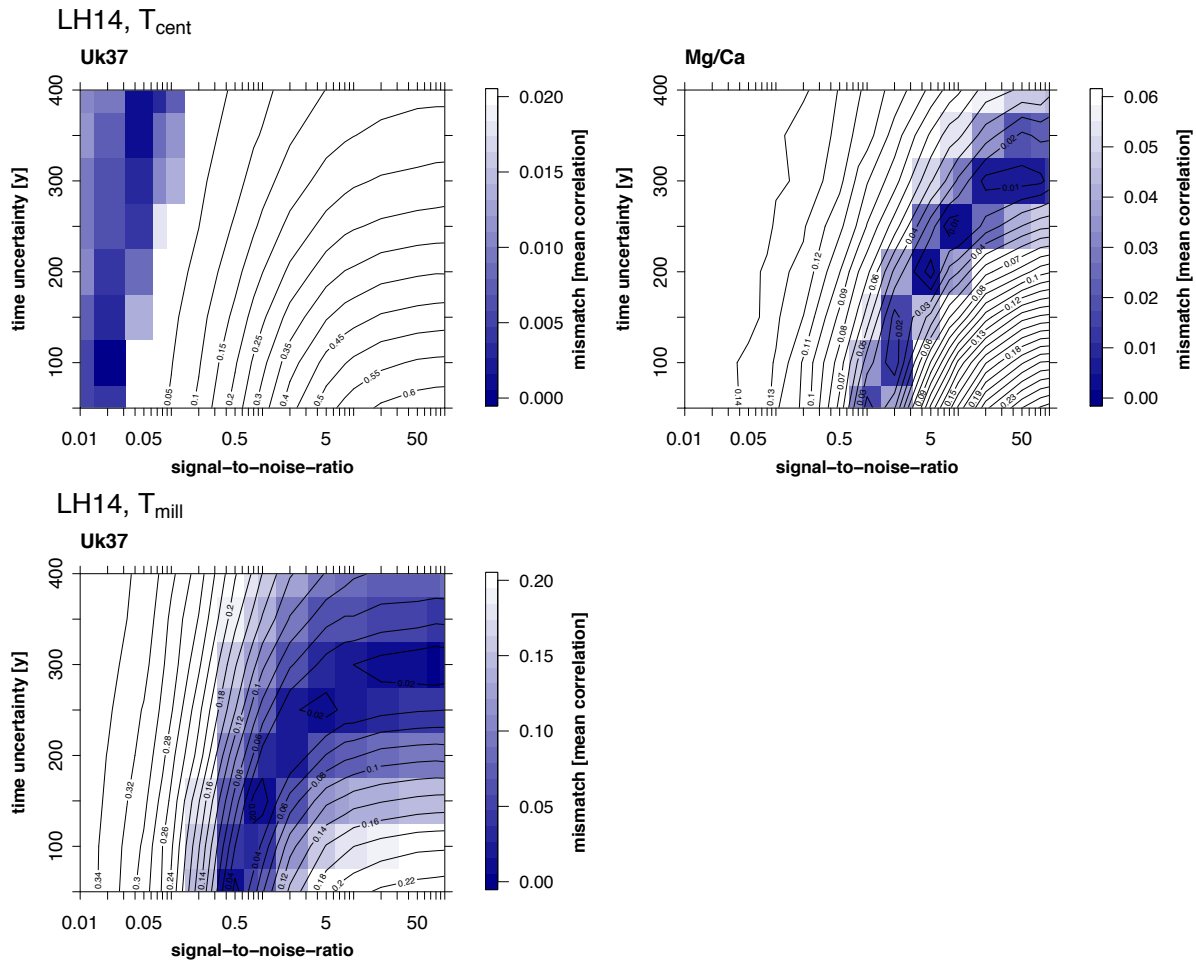


**Figure S14: Proxy-type-specific SNR estimates of Holocene temperature proxy records as a function of time uncertainty based on the LH14 dataset and related to centennial $T_{cent}$ and centennial to millennial time scales $T_{mill}$.** Each panel shows the mismatch between mean correlations of close-by (separation <5000 km) proxy records and model time series extracted from model T21k (TraCE-21ka model simulation) at proxy locations as a function of time uncertainty (vertical axis) and SNR (horizontal axis). Contour lines with numbers illustrate areas with the same mismatch. Coloured areas show the lowest mismatch and mark suitable combinations of SNR estimates and time uncertainties. On $T_{cent}$, Uk37-based estimates are low and Mg/Ca-based ones are high. $T_{mill}$ related SNR estimates for Mg/Ca are not possible as the mean correlations of the proxy time series are higher than the mean correlations of the model time series.

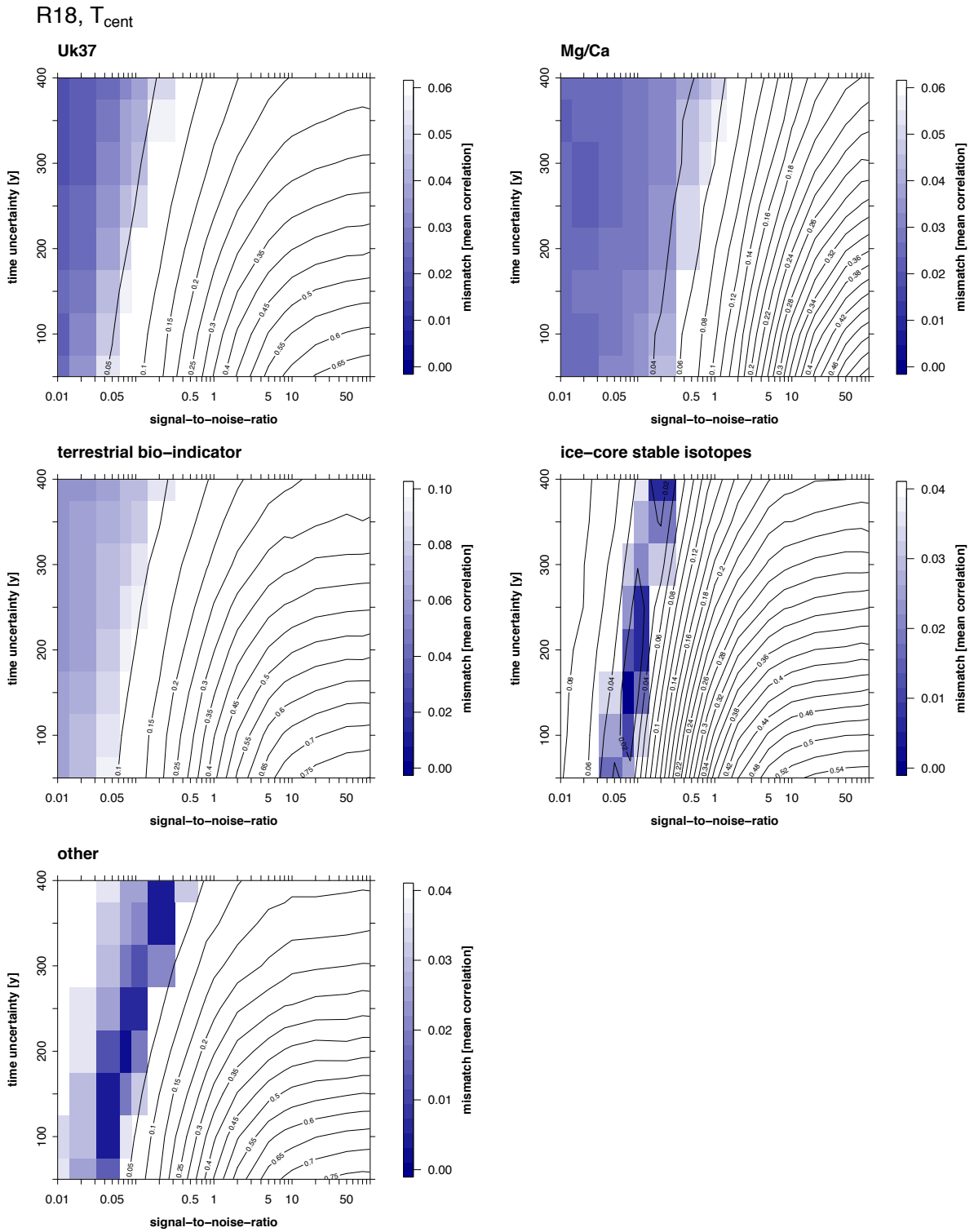


**Figure S15: Proxy-type-specific $SNR_{T21k,T_{cent}}$ estimates of Holocene temperature proxy records as a function of time uncertainty based on the R18 dataset and related to centennial time scales $T_{cent}$.** The panels illustrate the mismatch between mean correlations of close-by (separation <5000 km) proxy records and model time series extracted at proxy locations from model T21k (TraCE-21ka model simulation) as a function of time uncertainty (vertical axis) and SNR (horizontal axis). Contour lines with numbers mark parts with the same mismatch. Coloured areas highlight suitable combinations of SNR estimates and time uncertainties (lowest mismatch). All proxy types show (very) low $SNR_{T21k,T_{cent}}$ estimates.

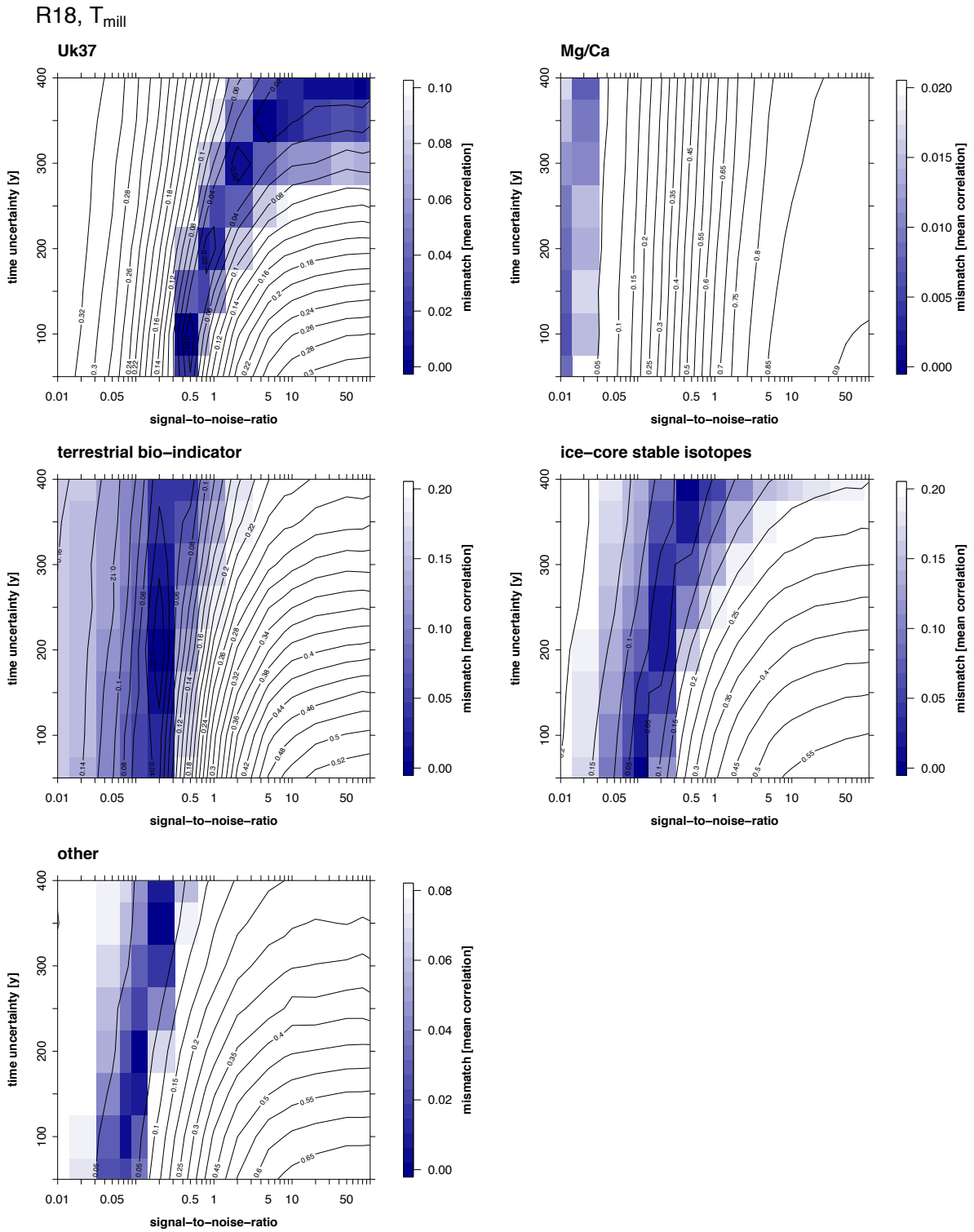


**Figure S16: Proxy-type-specific $SNR_{T21k,T_{mill}}$ estimates of Holocene temperature proxy records as a function of time uncertainty based on the R18 dataset and related to centennial to millennial time scales $T_{mill}$.** Each panel shows the mismatch between mean correlations of close-by (separation <5000 km) proxy records and model time series extracted at proxy locations from model T21k (TraCE-21ka model simulation) as a function of time uncertainty (vertical axis) and SNRs (horizontal axis). Contour lines mark parts with the same mismatch (numbers) and coloured areas (lowest mismatch) highlight suitable combinations of SNR estimates and time uncertainties. Most proxy-type-specific estimates show $SNR_{T21k,T_{mill}} < 0.5$.

## Supplementary Tables

**Table S1: List of records belonging to dataset M13.** The compilation is based on Marcott et al. (2013).

| Name | Lat [°N] | Lon [°E] | Archive | Proxy type | Reference |
|---|---|---|---|---|---|
| 17940 | 20.1 | 117.4 | marine sediment | Uk37 | Pelejero et al., 1999 |
| 18287-3 | 5.7 | 110.7 | marine sediment | Uk37 | Kienast et al., 2001 |
| 74KL | 14.3 | 57.3 | marine sediment | Uk37 | Huguet et al., 2006 |
| AD91-17 | 40.9 | 18.6 | marine sediment | Uk37 | Giunta et al., 2001 |
| CH07-98-GGC19 | 36.9 | -74.6 | marine sediment | Uk37 | Sachs, 2007 |
| Composite: MD01-2421; KR02-06 St. A GC; KR02-06 St. A MC | 36.0 | 141.8 | marine sediment | Uk37 | Isono et al., 2009 |
| D13882 | 38.6 | -9.5 | marine sediment | Uk37 | Rodrigues et al., 2009 |
| GeoB 1023-5 | -17.2 | 11.0 | marine sediment | Uk37 | Kim et al., 2002 |
| GeoB 3313-1 | -41.0 | -74.5 | marine sediment | Uk37 | Lamy et al., 2002 |
| GeoB 5844-2 | 27.7 | 34.7 | marine sediment | Uk37 | Arz et al., 2003 |
| GeoB 5901-2 | 36.4 | -7.1 | marine sediment | Uk37 | Kim et al., 2004 |
| GeoB 6518-1 | -5.6 | 11.2 | marine sediment | Uk37 | Schefuß et al., 2005 |
| IOW 225514 | 57.8 | 8.7 | marine sediment | Uk37 | Emeis et al., 2003 |
| IOW 225517 | 57.7 | 7.1 | marine sediment | Uk37 | Emeis et al., 2003 |
| JR51-GC35 | 67.0 | -18.0 | marine sediment | Uk37 | Bendle and Rosell-Melé, 2007 |
| M25/4-KL11 | 36.7 | 17.7 | marine sediment | Uk37 | Emeis et al., 2003 |
| M35003-4 | 12.1 | -61.3 | marine sediment | Uk37 | Rühlemann et al., 1999 |
| MD02-2529 | 8.2 | -84.1 | marine sediment | Uk37 | Leduc et al., 2007 |
| MD952011 | 67.0 | 7.6 | marine sediment | Uk37 | Calvo et al., 2002 |
| MD952015 | 58.8 | -26.0 | marine sediment | Uk37 | Marchal et al., 2002 |
| MD 95-2043 | 36.1 | -2.6 | marine sediment | Uk37 | Cacho et al., 2001 |
| MD97-2120 | -45.5 | 174.9 | marine sediment | Uk37 | Pahnke and Sachs, 2006 |
| MD97-2121 | -40.4 | 178.0 | marine sediment | Uk37 | Pahnke and Sachs, 2006 |
| NIOP905 | 10.8 | 51.9 | marine sediment | Uk37 | Huguet et al., 2006 |
| OCE326-GGC26 | 43.5 | -54.9 | marine sediment | Uk37 | Sachs, 2007 |
| OCE326-GGC30 | 43.9 | -62.8 | marine sediment | Uk37 | Sachs, 2007 |
| ODP Site 1019D | 41.7 | -124.9 | marine sediment | Uk37 | Barron et al., 2003 |
| SO136-GC11 | -43.4 | 167.9 | marine sediment | Uk37 | Barrows et al., 2007 |
| A7 | 27.8 | 127.0 | marine sediment | Mg/Ca | Sun et al., 2005 |
| BJ8-03-13GGC | -7.4 | 115.2 | marine sediment | Mg/Ca | Linsley et al., 2010 |
| BJ8-03-70GGC | -3.6 | 119.4 | marine sediment | Mg/Ca | Linsley et al., 2010 |
| GeoB 10038-4 | -5.9 | 103.3 | marine sediment | Mg/Ca | Mohtadi et al., 2010 |
| GeoB 3129 | -4.6 | -36.6 | marine sediment | Mg/Ca | Weldeab et al., 2006 |
| GeoB4905-4 | 2.5 | 9.4 | marine sediment | Mg/Ca | Weldeab et al., 2005 |
| KY07-04-01 | 31.6 | 128.9 | marine sediment | Mg/Ca | Kubota et al., 2010 |
| MD01-2378 | -13.1 | 121.8 | marine sediment | Mg/Ca | Xu et al., 2008 |
| MD01-2390 | 6.6 | 113.4 | marine sediment | Mg/Ca | Steinke et al., 2008 |
| MD02-2575 | 29.0 | -87.1 | marine sediment | Mg/Ca | Ziegler et al., 2008 |
| MD03-2707 | 2.5 | 9.4 | marine sediment | Mg/Ca | Weldeab et al., 2007 |
| MD98-2165 | -9.6 | 118.3 | marine sediment | Mg/Ca | Levi et al., 2007 |
| MD98-2176 | -5.0 | 133.4 | marine sediment | Mg/Ca | Stott et al., 2007 |
| MD98-2181 | 6.3 | 125.8 | marine sediment | Mg/Ca | Stott et al., 2007 |
| ME0005A-43JC | 7.9 | -83.6 | marine sediment | Mg/Ca | Benway et al., 2006 |
| ODP1084B | -25.5 | 13.0 | marine sediment | Mg/Ca | Farmer et al., 2005 |
| ODP 984 | 61.4 | -24.1 | marine sediment | Mg/Ca | Came et al., 2007 |
| PL07-39PC | 10.7 | -64.9 | marine sediment | Mg/Ca | Lea et al., 2003 |
| RAPID-12-1K | 62.1 | -17.8 | marine sediment | Mg/Ca | Thornalley et al., 2009 |

**Table S1:** (continued)

| Name | Lat [°N] | Lon [°E] | Archive | Proxy type | Reference |
|---|---|---|---|---|---|
| 74KL | 14.3 | 57.3 | marine sediment | $TEX_{86}$ | Huguet et al., 2006 |
| GeoB 7702-3 | 31.7 | 34.1 | marine sediment | $TEX_{86}$ | Castañeda et al., 2010 |
| NIOP905 | 10.8 | 51.9 | marine sediment | $TEX_{86}$ | Huguet et al., 2006 |
| NP04-KH04-3A-1K, -4A-1K | -6.7 | 29.8 | lacustrine sediment | $TEX_{86}$ | Tierney et al., 2008 |
| Flarken Lake | 58.6 | 13.7 | lacustrine sediment | Pollen MAT | Seppä et al. 2005 |
| Hanging Lake | 68.4 | -138.4 | lacustrine sediment | Chironomid transfer function | Kurek et al., 2009 |
| Homestead Scarp | -52.5 | 169.1 | lacustrine sediment | Pollen MAT | McGlone et al., 2010 |
| Lake 850 | 68.3 | 19.1 | lacustrine sediment | Chironomid transfer function | Larocque and Hall., 2004 |
| Lake Njulla | 68.4 | 18.7 | lacustrine sediment | Chironomid transfer function | Larocque and Hall., 2004 |
| Moose Lake | 61.4 | -143.6 | lacustrine sediment | Chironomid transfer function | Clegg et al., 2010 |
| Mount Honey | -52.6 | 169.1 | lacustrine sediment | Pollen MAT | McGlone et al., 2010 |
| Tsuolbmajavri Lake | 68.7 | 22.1 | lacustrine sediment | Pollen MAT | Seppä and Birks, 2001 |
| Agassiz & Renland | 80.7/ 71.3 | -73.1 / -26.7 | ice core | $\delta^{18}O$, borehole temp. | Vinther et al., 2009 |
| Dome F, Antarctica | -77.3 | 39.7 | ice core | $\delta^{18}O$, $\delta D$ | Kawamura et al., 2007 |
| EPICA Dome C, Antarctica | -75.1 | 123.4 | ice core | $\delta D$ | Jouzel et al., 2007 |
| EPICA DML | -75.0 | 0.1 | ice core | $\delta^{18}O$ | Stenni et al., 2010 |
| Vostok, Antarctica | -78.0 | 106.0 | ice core | $\delta D$ | Petit et al., 1999 |
| Composite: MD95-2011; HM79-4 | 67.0; 63.1 | 7.6; 2.6 | marine sediment | Radiolaria transfer function | Dolven et al., 2002 |
| GeoB 6518-1 | -5.6 | 11.2 | marine sediment | MBT | Weijers et al., 2007 |
| GIK23258-2 | 75.0 | 14.0 | marine sediment | Foram transfer function | Sarnthein et al., 2003 |
| MD79-257 | -20.4 | 36.3 | marine sediment | Foram MAT | Levi et al., 2007 |
| ODP 658C | 20.8 | -18.6 | marine sediment | Foram transfer function | deMenocal et al., 2000 |
| TN05-17 | -50.0 | 6.0 | marine sediment | Diatom MAT | Nielsen et al., 2004 |

**Table S2: List of records belonging to dataset LH14.** The compilation is based on Laepple and Huybers (2014).

| Name | Lat [°N] | Lon [°E] | Archive | Proxy type | Reference |
|---|---|---|---|---|---|
| CH07-98-GGC19 | 36.9 | -74.6 | marine sediment | Uk37 | Sachs, 2007 |
| D13882 | 38.6 | -9.5 | marine sediment | Uk37 | Rodrigues et al., 2009 |
| GeoB 3313-1 | -41.0 | -74.5 | marine sediment | Uk37 | Lamy et al., 2002 |
| GeoB 5901-2 | 36.4 | -7.1 | marine sediment | Uk37 | Kim et al., 2007 |
| GeoB 6007-2 | 30.9 | -10.3 | marine sediment | Uk37 | Kim et al., 2007 |
| IOW 225514 | 57.8 | 8.7 | marine sediment | Uk37 | Emeis et al., 2003 |
| IOW 225517 | 57.7 | 7.1 | marine sediment | Uk37 | Emeis et al., 2003 |
| JR51-GC35 | 67.0 | -18.0 | marine sediment | Uk37 | Bendle and Rosell-Melé, 2007 |
| KR02-06 | 36.0 | 141.8 | marine sediment | Uk37 | Isono et al., 2009 |
| MD01-2412 | 44.5 | 145.0 | marine sediment | Uk37 | Harada et al., 2006 |
| MD952011 | 67.0 | 7.6 | marine sediment | Uk37 | Calvo et al., 2002 |
| MD952015 | 58.8 | -26.0 | marine sediment | Uk37 | Marchal et al., 2002 |
| MD 95-2043 | 36.1 | -2.6 | marine sediment | Uk37 | Cacho et al., 2001 |
| MD972151 | 8.7 | 109.9 | marine sediment | Uk37 | Zhao et al., 2006 |
| OCE326-GGC26 | 43.5 | -54.9 | marine sediment | Uk37 | Sachs, 2007 |
| OCE326-GGC30 | 43.9 | -62.8 | marine sediment | Uk37 | Sachs, 2007 |
| ODP 658C | 20.8 | -18.6 | marine sediment | Uk37 | Zhao et al., 1995; deMenocal et al., 2000 |
| ODP Site 1019C | 41.7 | -124.9 | marine sediment | Uk37 | Barron et al., 2003 |
| SO139-74KL | -6.5 | 103.8 | marine sediment | Uk37 | Lückge et al., 2009 |
| SO90-39KG/56KA | 24.8 | 65.9 | marine sediment | Uk37 | Doose-Rolinski et al., 2001 |
| SSDP-102 | 35.0 | 128.9 | marine sediment | Uk37 | Kim et al., 2004 |
| A7 | 27.8 | 127.0 | marine sediment | Mg/Ca | Sun et al., 2005 |
| MD01-2378 | -13.1 | 121.8 | marine sediment | Mg/Ca | Xu et al., 2008 |
| MD03-2707 | 2.5 | 9.4 | marine sediment | Mg/Ca | Weldeab et al., 2007 |
| MD98-2176 | -5.0 | 133.4 | marine sediment | Mg/Ca | Stott et al., 2004 |
| MD98-2181 | 6.3 | 125.8 | marine sediment | Mg/Ca | Stott et al., 2004 |
| MD99-2251 | 57.4 | -27.9 | marine sediment | Mg/Ca | Farmer et al., 2008 |
| MD99-2203 | 35.0 | -75.2 | marine sediment | Mg/Ca | Cléroux et al., 2012 |
| MV99-GC41/PC14 | 25.2 | -112.7 | marine sediment | Mg/Ca | Marchitto et al., 2010 |
| ODP1084B | -25.5 | 13.0 | marine sediment | Mg/Ca | Farmer et al., 2005 |
| RAPID-12-1K | 62.1 | -17.8 | marine sediment | Mg/Ca | Thornalley et al., 2009 |

**Table S3: List of records belonging to dataset R18.** The compilation is based on Rehfeld et al. (2018).

| Name | Lat [°N] | Lon [°E] | Archive | Proxy type | Reference |
|---|---|---|---|---|---|
| CH07-98-GGC19 | 36.9 | -74.6 | marine sediment | Uk37 | Sachs, 2007 |
| D13882 | 38.6 | -9.5 | marine sediment | Uk37 | Rodrigues et al., 2010 |
| GeoB 3313-1 | -41.0 | -74.5 | marine sediment | Uk37 | Lamy et al., 2002 |
| GeoB 5901-2 | 36.4 | -7.1 | marine sediment | Uk37 | Kim et al., 2004 |
| GIK17940-2 | 20.1 | 117.4 | marine sediment | Uk37 | Pelejero et al., 1999 |
| IOW225514 | 57.8 | 8.7 | marine sediment | Uk37 | Emeis et al., 2003 |
| IOW225517 | 57.7 | 7.1 | marine sediment | Uk37 | Emeis et al., 2003 |
| Isono2009-Composite | 36.0 | 141.8 | marine sediment | Uk37 | Isono et al., 2009 |
| JR51-GC35 | 67.0 | -18.0 | marine sediment | Uk37 | Bendle and Rosell-Melé, 2007 |
| KNR195-5/ CDH 23 | -3.7 | -81.1 | marine sediment | Uk37 | Bova et al., 2015 |
| MD01-2412 | 44.5 | 145.0 | marine sediment | Uk37 | Harada et al., 2006 |
| MD01-2444 | 37.6 | -10.1 | marine sediment | Uk37 | Martrat et al., 2007 |
| MD03-2699 | 39.0 | -10.7 | marine sediment | Uk37 | Rodrigues et al., 2010 |
| MD952011 | 67.0 | 7.6 | marine sediment | Uk37 | Calvo et al., 2002 |
| MD952015 | 58.8 | -26.0 | marine sediment | Uk37 | Marchal et al., 2002 |
| MD 952043 | 36.1 | -2.6 | marine sediment | Uk37 | Cacho et al., 1999 |
| MD97-2120 | -45.5 | 174.9 | marine sediment | Uk37 | Pahnke and Sachs, 2006 |
| MD97-2121 | -40.4 | 178.0 | marine sediment | Uk37 | Pahnke and Sachs, 2006 |
| MD982195 | 31.6 | 128.9 | marine sediment | Uk37 | Ijiri et al., 2005 |
| NIOP905 | 10.8 | 51.9 | marine sediment | Uk37 | Huguet et al., 2006 |
| OCE326-GGC26 | 43.5 | -54.9 | marine sediment | Uk37 | Sachs, 2007 |
| OCE326-GGC30 | 43.9 | -62.8 | marine sediment | Uk37 | Sachs, 2007 |
| ODP 658C | 20.8 | -18.6 | marine sediment | Uk37 | Zhao et al., 1995 |
| ODP Site 1019C | 41.7 | -124.9 | marine sediment | Uk37 | Barron et al., 2003 |
| P178-15P-uk37 | 12.0 | 44.3 | marine sediment | Uk37 | Tierney et al., 2016 |
| PC6 | 40.4 | 143.5 | marine sediment | Uk37 | Minoshima et al., 2007 |
| SO139-74KL | -6.5 | 103.8 | marine sediment | Uk37 | Lückge et al., 2009 |
| A7 | 27.8 | 127.0 | marine sediment | Mg/Ca | Sun et al., 2005 |
| BJ8-03-13GGC | -7.4 | 115.2 | marine sediment | Mg/Ca | Linsley et al., 2010 |
| BJ8-03-70GGC | -3.6 | 119.4 | marine sediment | Mg/Ca | Linsley et al., 2010 |
| GeoB 3129 | -4.6 | -36.6 | marine sediment | Mg/Ca | Weldeab et al., 2006 |
| KY07-04-01 | 31.6 | 128.9 | marine sediment | Mg/Ca | Kubota et al., 2010 |
| MD01-2378 | -13.1 | 121.8 | marine sediment | Mg/Ca | Xu et al., 2008 |
| MD01-2390 | 6.6 | 113.4 | marine sediment | Mg/Ca | Steinke et al., 2008 |
| MD03-2707 | 2.5 | 9.4 | marine sediment | Mg/Ca | Weldeab et al., 2007 |
| MD98-2165 | -9.6 | 118.3 | marine sediment | Mg/Ca | Levi et al., 2007 |
| MD98-2176 | -5.0 | 133.4 | marine sediment | Mg/Ca | Stott et al., 2007 |
| MD98-2181 | 6.3 | 125.8 | marine sediment | Mg/Ca | Stott et al., 2002 |
| ODP1084B | -25.5 | 13.0 | marine sediment | Mg/Ca | Farmer et al., 2005 |
| ODP 1240 | 0.0 | -86.5 | marine sediment | Mg/Ca | Pena et al., 2008 |
| ODP 984 | 61.4 | -24.1 | marine sediment | Mg/Ca | Came et al., 2007 |
| P178-15P-mgca | 12.0 | 44.3 | marine sediment | Mg/Ca | Tierney et al., 2016 |
| PL07-39PC | 10.7 | -64.9 | marine sediment | Mg/Ca | Lea et al., 2003 |
| RAPID-12-1K | 62.1 | -17.8 | marine sediment | Mg/Ca | Thornalley et al., 2009 |
| SK237-GC04 | 11.0 | 75.0 | marine sediment | Mg/Ca | Saraswat et al., 2013 |
| SO189-39KL | -0.8 | 99.9 | marine sediment | Mg/Ca | Mohtadi et al., 2014 |

**Table S3:** (continued)

| Name | Lat [°N] | Lon [°E] | Archive | Proxy type | Reference |
|---|---|---|---|---|---|
| GeoB 7702-3 | 31.7 | 34.1 | marine sediment | $TEX_{86}$ | Castañeda et al., 2010 |
| Lake Tanganyika | -6.7 | 29.8 | lacustrine sediment | $TEX_{86}$ | Tierney et al., 2008 |
| NIOP905 | 10.8 | 51.9 | marine sediment | $TEX_{86}$ | Huguet et al., 2006 |
| P178-15P-tex86 | 12.0 | 44.3 | marine sediment | $TEX_{86}$ | Tierney et al., 2016 |
| Dyer | 66.6 | -61.4 | lacustrine sediment | Pollen Assemblage | Gajewski, 2015 |
| Flarken Lake | 58.6 | 13.7 | lacustrine sediment | Pollen Assemblage | Seppä et al., 2005 |
| Hanging Lake | 68.4 | -138.4 | lacustrine sediment | Chironomid Assemblage | Kurek et al., 2009 |
| JR01 | 69.9 | -95.1 | lacustrine sediment | Pollen Assemblage | Gajewski, 2015 |
| KR02 | 71.3 | -113.8 | lacustrine sediment | Pollen Assemblage | Gajewski, 2015 |
| Lake31 | 67.1 | -50.5 | lacustrine sediment | Pollen Assemblage | Gajewski, 2015 |
| Lake 850 | 68.3 | 19.1 | lacustrine sediment | Chironomid Assemblage | Larocque and Bigler, 2004 |
| Lake Njulla | 68.4 | 18.7 | lacustrine sediment | Chironomid Assemblage | Bigler et al., 2003 |
| Moose Lake | 61.4 | -143.6 | lacustrine sediment | Chironomid Assemblage | Clegg et al., 2010 |
| ODP 976-4 | 36.2 | -4.3 | marine sediment | Pollen Assemblage | Combourieu-Nebout et al., 2009 |
| Tsuolbmajavri Lake | 68.7 | 22.1 | lacustrine sediment | Pollen Assemblage | Seppä and Birks, 2001 |
| Agassiz 84/87 | 80.7 | -73.1 | ice core | $\delta^{18}O$ | Koerner and Fisher, 1990; Vinther et al., 2009 |
| Byrd | -80.0 | -119.5 | ice core | $\delta^{18}O$ | Epstein et al., 1970; WAIS Divide Project Members, 2013 |
| Camp Century | 77.2 | -61.1 | ice core | $\delta^{18}O$ | Dansgaard et al., 1969; Vinther et al., 2009 |
| Dome C | -74.7 | 124.2 | ice core | $\delta^{18}O$ | Lorius et al., 1979 |
| Dome F | -77.3 | 39.7 | ice core | $\delta^{18}O$ | Watanabe et al., 1999, 2003; Uemura et al., 2012 |
| DYE 3 | 65.2 | -43.8 | ice core | $\delta^{18}O$ | Dansgaard et al., 1982; Vinther et al., 2009 |
| EPICA DML | -75.0 | 0.0 | ice core | $\delta^{18}O$ | EPICA Community Members, 2006; Veres et al., 2013 |
| EPICA Dome C | -75.1 | 123.4 | ice core | $\delta^{2}H$ | EPICA Community Members, 2004; Jouzel et al., 2007; Veres et al., 2013 |
| GISP2 | 72.6 | -38.5 | ice core | $\delta^{18}O$ | Grootes et al., 1993; Grootes and Stuiver, 1997; Stuiver and Grootes, 2000; Seierstad et al., 2014 |
| GRIP | 72.6 | -37.6 | ice core | $\delta^{18}O$ | Johnsen et al., 1992, 1997; Seierstad et al., 2014 |
| Huascaran | -9.1 | -77.6 | ice core | $\delta^{18}O$ | Thompson et al., 1995 |

**Table S3:** (continued)

| Name | Lat [°N] | Lon [°E] | Archive | Proxy type | Reference |
|---|---|---|---|---|---|
| NGRIP | 75.1 | -42.3 | ice core | $\delta^{18}O$ | NGRIP Members, 2004; Veres et al., 2013 |
| Penny Ice Cap | 67.3 | -65.8 | ice core | $\delta^{18}O$ | Fisher et al., 1998 |
| Siple Dome | -81.7 | -148.8 | ice core | $\delta^{18}O$ | Taylor et al., 2004; WAIS Devide Project Members, 2013 |
| Talos Dome | -72.8 | 159.1 | ice core | $\delta^{18}O$ | Stenni et al., 2011; Veres et al., 2013 |
| Taylor Dome | -77.8 | 158.7 | ice core | $\delta^{18}O$ | Steig et al., 2000 |
| Vostok | -78.0 | 106.0 | ice core | $\delta^{2}H$ | Petit et al., 1999; Veres et al., 2013 |
| WAIS Divide | -79.5 | -112.1 | ice core | $\delta^{18}O$ | WAIS Devide Project Members, 2013 |
| GeoB 6518-1 | -5.6 | 11.2 | marine sediment | MBT/CBT | Weijers et al., 2007 |
| GreatBasin | 38.0 | -116.5 | tree | ring width | Salzer et al., 2014 |
| Kangerlussuaq-Stack | 67.0 | -50.7 | lacustrine sediment | Uk37 | D'Andrea et al., 2011 |
| MD95-2011 | 67.0 | 7.6 | marine sediment | Foraminiferal Assemblage | Risebrobakken et al., 2003 |
| MD95-2011 | 67.0 | 7.6 | marine sediment | Radiolarian Assemblage | Dolven et al., 2002 |
| MD99-2275 | 66.6 | -17.7 | marine sediment | Diatom Assemblage | Jiang et al., 2015 |
| NA 87-22 | 55.5 | -14.7 | marine sediment | Foraminiferal Assemblage | Waelbroeck et al., 2001 |
| ODP 658C | 20.8 | -18.6 | marine sediment | Foraminiferal Assemblage | deMenocal et al., 2000 |
| Qinghai | 36.8 | 100.1 | lacustrine sediment | Uk37 | Hou et al., 2016 |

**Table S4: Number of record pairs for different proxy types used for the SNR estimation (pairs of time series with separation distances <5000 km).** The number of records pairs is given in total (independent of proxy type) and separated per proxy type for each proxy compilation. $T_{mill}$ refers to the number of pairs of time series with a mean inter-observation time step of $\Delta t$ <500y and $T_{cent}$ counts pairs of time series with $\Delta t$ <200y.

| | **All proxy types** | **Uk37** | **Mg/Ca** | **$TEX_{86}$** | **Terrestrial bio-indicator** | **Ice-core stable isotopes** | **other** |
|---|---|---|---|---|---|---|---|
| M13 – $T_{mill}$ | 497 | 99 | 52 | 6 | 11 | 6 | 5 |
| M13 – $T_{cent}$ | 312 | 59 | 37 | - | 11 | 3 | 1 |
| LH14 – $T_{mill}$ | 141 | 75 | 11 | - | - | - | - |
| LH14 – $T_{cent}$ | 141 | 75 | 11 | - | - | - | - |
| R18 – $T_{mill}$ | 939 | 96 | 53 | 6 | 45 | 66 | 12 |
| R18 – $T_{cent}$ | 862 | 95 | 51 | 1 | 39 | 66 | 11 |

**Supplementary References**


Arz, H. W., Pätzold, J., Müller, P. J., and Moammar, M. O.: Influence of Northern Hemisphere climate and global sea level rise on the restricted Red Sea marine environment during termination I, Paleoceanography, 18(2), 1053, doi:10.1029/2002PA000864, 2003.

Barron, J. A., Heusser, L., Herbert, T., and Lyle, M.: High-resolution climatic evolution of coastal northern California during the past 16,000 years, Paleoceanography, 18(1), 1020, doi:10.1029/2002PA000768, 2003.

Barrows, T. T., Lehman, S. J., Fifield, L. K., and De Deckker, P.: Absence of Cooling in New Zealand and the Adjacent Ocean During the Younger Dryas Chronozone, Science, 318(5847), 86-89, doi:10.1126/science.1145873, 2007.

Bendle, J. A. P., and Rosell-Melé, A.: High-resolution alkenone sea surface temperature variability on the North Icelandic Shelf: implications for Nordic Seas palaeoclimatic development during the Holocene, The Holocene, 17(1), 9-24, doi:10.1177/0959683607073269, 2007.

Benway, H. M., Mix, A. C., Haley, B. A., and Klinkhammer, G. P.: Eastern Pacific Warm Pool paleosalinity and climate variability: 0–30 kyr, Paleoceanography, 21, PA3008, doi:10.1029/2005PA001208, 2006.

Bigler, C., Grahn, E., Larocque, I., Jeziorski, A., and Hall, R.: Holocene environmental change at Lake Njulla (999 m a.s.l.), northern Sweden: a comparison with four small nearby lakes along an altitudinal gradient, J. Paleolimnol., 29, 13-29, 2003.

Bova, S. C., Herbert, T., Rosenthal, Y., Kalansky, J., Altabet, M., Chazen, C., Mojarro, A., and Zech, J.: Links between eastern equatorial Pacific stratification and atmospheric CO2 rise during the last deglaciation, Paleoceanography, 30, 1407-1424, doi:10.1002/2015PA002816, 2015.

Cacho, I., Grimalt, J. O., Pelejero, C., Canals, M., Sierro, F. J., Flores, J. A., and Shackleton, N.: Dansgaard-Oeschger and Heinrich event imprints in Alboran Sea paleotemperatures, Paleoceanography, 14(6), 698-705, 1999.

Cacho, I., Grimalt, J. O., Canals, M., Sbaffi, L., Shackleton, N. J., Schönfeld, J., and Zahn, R.: Variability of the western Mediterranean Sea surface temperature during the last 25,000 years and its connection with the Northern Hemisphere climatic changes, Paleoceanography, 16(1), 40-52, 2001.

Calvo, E., Grimalt, J., and Jansen, E.: High resolution UK37 sea surface temperature reconstruction in the Norwegian Sea during the Holocene, Quaternary Sci. Rev., 21, 1385-1394, 2002.

Came, R. E., Oppo, D. W., and McManus, J. F.: Amplitude and timing of temperature and salinity variability in the subpolar North Atlantic over the past 10 k.y., Geology, 35(4), 315-318, doi:10.1130/G23455A.1, 2007.

Castañeda, I. S., Schefuß, E., Pätzold, J., Damsté, J. S. S., Weldeab, S., and Schouten, S.: Millennial-scale sea surface temperature changes in the eastern Mediterranean (Nile River Delta region) over the last 27,000 years, Paleoceanography, 25, PA1208, doi:10.1029/2009PA001740, 2010.

Clegg, B. F., Clarke, G. H., Chipman, M. L., Chou, M., Walker, I. R., Tinner, W., and Hu, F. S.: Six millennia of summer temperature variation based on midge analysis of lake sediments from Alaska, Quaternary Sci. Rev., 29, 3308-3316, doi:10.1016/j.quascirev.2010.08.001, 2010.

Cléroux, C., Debret, M., Cortijo, E., Duplessy, J.-C., Dewilde, F., Reijmer, J., and Massei, N.: High-resolution sea surface reconstructions off Cape Hatteras over the last 10 ka, Paleoceanography, 27, PA1205, doi:10.1029/2011PA002184, 2012.

Combourieu-Nebout, N., Peyron, O., Dormoy, I., Desprat, S., Beaudouin, C., Kotthoff, U., and Marret, F.: Rapid climatic variability in the west Mediterranean during the last 25 000 years from high resolution pollen data, Clim. Past, 5, 503-521, 2009.

Compo, G. P., Whitaker, J. S., and Sardeshmukh, P. D.: Feasibility of a 100-year reanalysis using only surface pressure data, B. Am. Meteorol. Soc., 87(2), 175-190, doi:10.1175/BAMS-87-2-175, 2006.

D'Andrea, W. J., Huang, Y., Fritz, S. C., and Anderson, N. J.: Abrupt Holocene climate change as an important factor for human migration in West Greenland, P. Natl. Acad. Sci. USA, 108(24), 9765-9769, doi:10.1073/pnas.1101708108, 2011.

Dansgaard, W., Johnsen, S. J., Møller, J., and Langway, C. C.: One Thousand Centuries of Climatic Record from Camp Century on the Greenland Ice Sheet, Science, 166(3903), 377-380, doi:10.1126/science.166.3903.377, 1969.

Dansgaard, W., Clausen, H. B., Gundestrup, N., Hammer, C. U., Johnsen, S. F., Kristinsdottir, P. M., and Reeh, N.: A New Greenland Deep Ice Core, Science, 218(4579), 1273-1277, doi:10.1126/science.218.4579.1273, 1982.

deMenocal, P., Ortiz, J., Guilderson, T., and Sarnthein, M.: Coherent High- and Low-Latitude Climate Variability During the Holocene Warm Period, Science, 288(5474), 2198-2202, doi:10.1126/science.288.5474.2198, 2000.

Dolven, J. K., Cortese, G., and Bjørklund, K. R.: A high-resolution radiolarian-derived paleotemperature record for the Late Pleistocene-Holocene in the Norwegian Sea, Paleoceanography, 17(4), 1072, doi:10.1029/2002PA000780, 2002.

Doose-Rolinski, H., Rogalla, U., Scheeder, G., Lückge, A., and von Rad, U.: High-resolution temperature and evaporation changes during the late Holocene in the northeastern Arabian Sea, Paleoceanography, 16(4), 358-367, 2001.

Emeis, K.-C., Struck, U., Blanz, T., Kohly, A., and Voβ, M.: Salinity changes in the central Baltic Sea (NW Europe) over the last 10 000 years, The Holocene, 13(3), 411-421, doi:10.1191/0959683603hl634rp, 2003.

EPICA Community Members: Eight glacial cycles from an Antarctic ice core, Nature, 429, 623-628, doi:10.1038/nature02599, 2004.

EPICA Community Members: One-to-one coupling of glacial climate variability in Greenland and Antarctica, Nature, 444, 195-198, doi:10.1038/nature05301, 2006.

Epstein, S., Sharp, R. P., and Gow, A. J.: Antarctic Ice Sheet: Stable Isotope Analyses of Byrd Station Cores and Interhemispheric Climatic Implications, Science, 168(3939), 1570-1572, doi:10.1126/science.168.3939.1570, 1970.

Farmer, E. C., deMenocal, P. B., and Marchitto, T. M.: Holocene and deglacial ocean temperature variability in the Benguela upwelling region: Implications for low-latitude atmospheric circulation, Paleoceanography, 20, PA2018, doi:10.1029/2004PA001049, 2005.

Farmer, E. J., Chapman, M. R., and Andrews, J. E.: Centennial-scale Holocene North Atlantic surface temperatures from Mg/Ca ratios in Globigerina bulloides, Geochem. Geophys. Geosyst., 9, Q12029, doi:10.1029/2008GC002199, 2008.

Fisher, D. A., Koerner, R. M., Bourgeois, J. C., Zielinski, G., Wake, C., Hammer, C. U., Clausen, H. B., Gundestrup, N., Johnsen, S., Goto-Azuma, K., Hondoh, T., Blake, E., and Gerasimoff, M.: Penny Ice Cap Cores, Baffin Island, Canada, and the Wisconsinan Foxe Dome Connection: Two States of Hudson Bay Ice Cover, Science, 279(5351), 692-695, doi:10.1126/science.279.5351.692, 1998.

Gajewski, K.: Quantitative reconstruction of Holocene temperatures across the Canadian Arctic and Greenland, Global Planet. Change, 128, 14-23, doi:10.1016/j.gloplacha.2015.02.003, 2015.

Giunta, S., Emeis, K.-C., and Negri, A.: Sea surface temperatures reconstruction of the last 16,000 years in the Eastern Mediterranean Sea, Riv. Ital. Paleontol. S., 107(3), 463-476, 2001.

Grootes, P. M., and Stuiver, M.: Oxygen 18/16 variability in Greenland snow and ice with 10− 3- to 105-year time resolution, J. Geophys. Res., 102(C12), 26455-26470, 1997.

Grootes, P. M., Stuiver, M., White, J. W. C., Johnsen, S., and Jouzel, J.: Comparison of oxygen isotope records from the GISP2 and GRIP Greenland ice cores, Nature, 366, 552-554, 1993.

Harada, N., Ahagon, N., Sakamoto, T., Uchida, M., Ikehara, M., and Shibata, Y.: Rapid fluctuation of alkenone temperature in the southwestern Okhotsk Sea during the past 120 ky, Global Planet. Change, 53, 29-46, doi:10.1016/j.gloplacha.2006.01.010, 2006.

Hou, J., Huang, Y., Zhao, J., Liu, Z., Colman, S., and An, Z.: Large Holocene summer temperature oscillations and impact on the peopling of the northeastern Tibetan Plateau, Geophys. Res. Lett., 43, 1323-1330, doi:10.1002/2015GL067317, 2016.

Huguet, C., Kim, J.-H., Damsté, J. S. S., and Schouten, S.: Reconstruction of sea surface temperature variations in the Arabian Sea over the last 23 kyr using organic proxies (TEX86 and UK′37), Paleoceanography, 21, PA3003, doi:10.1029/2005PA001215, 2006.

Ijiri, A., Wang, L., Oba, T., Kawahata, H., Huang, C.-Y., and Huang, C.-Y.: Paleoenvironmental changes in the northern area of the East China Sea during the past 42,000 years, Palaeogeogr. Palaeocl., 219, 239-261, doi:10.1016/j.palaeo.2004.12.028, 2005.

Isono, D., Yamamoto, M., Irino, T., Oba, T., Murayama, M., Nakamura, T., and Kawahata, H.: The 1500-year climate oscillation in the midlatitude North Pacific during the Holocene, Geology, 37(7), 591-594, doi:10.1130/G25667A.1, 2009.

Jiang, H., Muscheler, R., Björck, S., Seidenkrantz, M.-S., Olsen, J., Sha, L., Sjolte, J., Eiríksson, J., Ran, L., Knudsen, K.-L., and Knudsen, M. F.: Solar forcing of Holocene summer sea-surface temperatures in the northern North Atlantic, Geology, 43(3), 203-206, doi:10.1130/G36377.1, 2015.

Johnsen, S. J., Clausen, H. B., Dansgaard, W., Fuhrer, K., Gundestrup, N., Hammer, C. U., Iversen, P., Jouzel, J., Stauffer, B., and Steffensen, J. P.: Irregular glacial interstadials recorded in a new Greenland ice core, Nature, 359, 311-313, 1992.

Johnsen, S. J., Clausen, H. B., Dansgaard, W., Gundestrup, N. S., Hammer, C. U., Andersen, U., Anderson, K. K., Hvidberg, C. S., Dahl-Jensen, D., Steffensen, J. P., Shoji, H., Sveinbjörnsdóttir, Á. E., White, J., Jouzel, J., and Fisher, D.: The δ18O record along the Greenland Ice Core Project deep ice core and the problem of possible Eemian climatic instability, J. Geophys. Res., 102(C12), 26397-26410, 1997.

Jouzel, J., Masson-Delmotte, V., Cattani, O., Dreyfus, G., Falourd, S., Hoffmann, G., Minster, B., Nouet, J., Barnola, J. M., Chappellaz, J., Fischer, H., Gallet, J. C., Johnsen, S., Leuenberger, M., Loulergue, L., Luethi, D., Oerter, H., Parrenin, F., Raisbeck, G., Raynaud, D., Schilt, A., Schwander, J., Selmo, E., Souchez, R., Spahni, R., Stauffer, B., Steffensen, J. P., Stenni, B., Stocker, T. F., Tison, J. L., Werner, M., and Wolff, E. W.: Orbital and Millennial Antarctic Climate Variability over the Past 800,000 Years, Science, 317(5839), 793-796, doi:10.1126/science.1141038, 2007.

Kawamura, K., Parrenin, F., Lisiecki, L., Uemura, R., Vimeux, F., Severinghaus, J. P., Hutterli, M. A., Nakazawa, T., Aoki, S., Jouzel, J., Raymo, M. E., Matsumoto, K., Nakata, H., Motoyama, H., Fujita, S., Goto-Azuma, K., Fujii, Y., and Watanabe, O.: Northern Hemisphere forcing of climatic cycles in Antarctica over the past 360,000 years, Nature, 448, 912-916, doi:10.1038/nature06015, 2007.

Kienast, M., Steinke, S., Stattegger, K., and Calvert, S. E.: Synchronous Tropical South China Sea SST Change and Greenland Warming During Deglaciation, Science, 291(5511), 2132-2134, doi:10.1126/science.1057131, 2001.

Kim, J.-H., Schneider, R. R., Müller, P. J., and Wefer, G.: Interhemispheric comparison of deglacial sea-surface temperature patterns in Atlantic eastern boundary currents, Earth Planet. Sc. Lett., 194, 383-393, 2002.

Kim, J.-H., Rimbu, N., Lorenz, S. J., Lohmann, G., Nam, S.-I., Schouten, S., Rühlemann, C., and Schneider, R. R.: North Pacific and North Atlantic sea-surface temperature variability during the Holocene, Quaternary Sci. Rev., 23, 2141-2154, doi:10.1016/j.quascirev.2004.08.010, 2004.

Kim, J.-H., Meggers, H., Rimbu, N., Lohmann, G., Freudenthal, T., Müller, P. J., and Schneider, R. R.: Impacts of the North Atlantic gyre circulation on Holocene climate off northwest Africa, Geology, 35(5), 387-390, doi:10.1130/G23251A.1, 2007.

Koerner, R. M., and Fisher, D. A.: A record of Holocene summer climate from a Canadian high-Arctic ice core, Nature, 343, 630-631, 1990.

Kubota, Y., Kimoto, K., Tada, R., Oda, H., Yokoyama, Y., and Matsuzaki, H.: Variations of East Asian summer monsoon since the last deglaciation based on Mg/Ca and oxygen isotope of planktic foraminifera in the northern East China Sea, Paleoceanography, 25, PA4205, doi:10.1029/2009PA001891, 2010.

Kurek, J., Cwynar, L. C., and Vermaire, J. C.: A late Quaternary paleotemperature record from Hanging Lake, northern Yukon Territory, eastern Beringia, Quaternary Res., 72, 246-257, doi:10.1016/j.yqres.2009.04.007, 2009.

Laepple, T., and Huybers, P.: Ocean surface temperature variability: Large model–data differences at decadal and longer periods, P. Natl. Acad. Sci. USA, 111(47), 16682-16687, doi:10.1073/pnas.1412077111, 2014.

Lamy, F., Rühlemann, C., Hebbeln, D., and Wefer, G.: High- and low-latitude climate control on the position of the southern Peru-Chile Current during the Holocene, Paleoceanography, 17(2), 1028, doi:10.1029/2001PA000727, 2002.

Larocque, I., and Bigler, C.: Similarities and discrepancies between chironomid- and diatom-inferred temperature reconstructions through the Holocene at Lake 850, northern Sweden, Quatern. Int., 122, 109-121, doi:10.1016/j.quaint.2004.01.033, 2004.

Larocque, I., and Hall, R. I.: Holocene temperature estimates and chironomid community composition in the Abisko Valley, northern Sweden, Quaternary Sci. Rev., 23, 2453-2465, doi:10.1016/j.quascirev.2004.04.006, 2004.

Lea, D. W., Pak, D. K., Peterson, L. C., and Hughen, K. A.: Synchroneity of Tropical and High-Latitude Atlantic Temperatures over the Last Glacial Termination, Science, 301(5638), 1361-1364, doi:10.1126/science.1088470, 2003.

Leduc, G., Vidal, L., Tachikawa, K., Rostek, F., Sonzogni, C., Beaufort, L., and Bard, E.: Moisture transport across Central America as a positive feedback on abrupt climatic changes, Nature, 445, 908-911, doi:10.1038/nature05578, 2007.

Levi, C., Labeyrie, L., Bassinot, F., Guichard, F., Cortijo, E., Waelbroeck, C., Caillon, N., Duprat, J., de Garidel-Thoron, T., and Elderfield, H.: Low-latitude hydrological cycle and rapid climate changes during the last deglaciation, Geochem. Geophys. Geosyst., 8(5), doi:10.1029/2006GC001514, 2007.

Linsley, B. K., Rosenthal, Y., and Oppo, D. W.: Holocene evolution of the Indonesian throughflow and the western Pacific warm pool, Nat. Geosci., 3, 578-583, doi:10.1038/NGEO920, 2010.

Lorius, C., Merlivat, L., Jouzel, J., and Pourchet, M.: A 30,000-yr isotope climatic record from Antarctic ice, Nature, 280, 644-648, 1979.

Lückge, A., Mohtadi, M., Rühlemann, C., Scheeder, G., Vink, A., Reinhardt, L., and Wiedicke, M.: Monsoon versus ocean circulation controls on paleoenvironmental conditions off southern Sumatra during the past 300,000 years, Paleoceanography, 24, PA1208, doi:10.1029/2008PA001627, 2009.

Marchal, O., Cacho, I., Stocker, T. F., Grimalt, J. O., Calvo, E., Martrat, B., Shackleton, N., Vautravers, M., Cortijo, E., van Kreveld, S., Andersson, C., Koc, N., Chapman, M., Sbaffi, L., Duplessy, J.-C., Sarnthein, M., Turon, J.-L., Duprat, J., and Jansen, E.: Apparent long-term cooling of the sea surface in the northeast Atlantic and Mediterranean during the Holocene, Quaternary Sci. Rev., 21, 455-483, 2002.

Marchitto, T. M., Muscheler, R., Ortiz, J. D., Carriquiry, J. D., and van Geen, A.: Dynamical Response of the Tropical Pacific Ocean to Solar Forcing During the Early Holocene, Science, 330(6009), 1378-1381, doi:10.1126/science.1194887, 2010.

Marcott, S. A., Shakun, J. D., Clark, P. U., and Mix, A. C.: A Reconstruction of Regional and Global Temperature for the Past 11,300 Years, Science, 339(6124), 1198-1201, doi:10.1126/science.1228026, 2013.

Martrat, B., Grimalt, J. O., Shackleton, N. J., de Abreu, L., Hutterli, M. A., and Stocker, T. F.: Four Climate Cycles of Recurring Deep and Surface Water Destabilizations on the Iberian Margin, Science, 317(5837), 502-507, doi:10.1126/science.1139994, 2007.

McGlone, M. S., Turney, C. S. M., Wilmshurst, J. M., Renwick, J., and Pahnke, K.: Divergent trends in land and ocean temperature in the Southern Ocean over the past 18,000 years, Nat. Geosci., 3, 622-626, doi:10.1038/NGEO931, 2010.

Minoshima, K., Kawahata, H., and Ikehara, K.: Changes in biological production in the mixed water region (MWR) of the northwestern North Pacific during the last 27 kyr, Palaeogeogr. Palaeocl., 254, 430-447, doi:10.1016/j.palaeo.2007.06.022, 2007.

Mohtadi, M., Steinke, S., Lückge, A., Groeneveld, J., and Hathorne, E. C.: Glacial to Holocene surface hydrography of the tropical eastern Indian Ocean, Earth Planet. Sc. Lett., 292, 89-97, doi:10.1016/j.epsl.2010.01.024, 2010.

Mohtadi, M., Prange, M., Oppo, D. W., De Pol-Holz, R., Merkel, U., Zhang, X., Steinke, S., and Lückge, A.: North Atlantic forcing of tropical Indian Ocean climate, Nature, 509, 76-80, doi:10.1038/nature13196, 2014.

NGRIP Members: High-resolution record of Northern Hemisphere climate extending into the last interglacial period, Nature, 431, 147-151, doi:10.1038/nature02805, 2004.

Nielsen, S. H., Koç, N., and Crosta, X.: Holocene climate in the Atlantic sector of the Southern Ocean: Controlled by insolation or oceanic circulation?, Geology, 32(4), 317-320, doi:10.1130/G20334.1, 2004.

Pahnke, K., and Sachs, J. P.: Sea surface temperatures of southern midlatitudes 0–160 kyr B.P., Paleoceanography, 21, PA2003, doi:10.1029/2005PA001191, 2006.

Pelejero, C., Grimalt, J. O., Heilig, S., Kienast, M., and Wang, L.: High-resolution UK37 temperature reconstructions in the South China Sea over the past 220 kyr, Paleoceanography, 14(2), 224-231, 1999.

Pena, L. D., Cacho, I., Ferretti, P., and Hall, M. A.: El Niño–Southern Oscillation–like variability during glacial terminations and interlatitudinal teleconnections, Paleoceanography, 23, PA3101, doi:10.1029/2008PA001620, 2008.

Petit, J. R., Jouzel, J., Raynaud, D., Barkov, N. I., Barnola, J.-M., Basile, I., Bender, M., Chappellaz, J., Davis, M., Delaygue, G., Delmotte, M., Kotlyakov, V. M., Legrand, M., Lipenkov, V. Y., Lorius, C., Pépin, L., Ritz, C., Saltzman, E., and Stievenard, M.: Climate and atmospheric history of the past 420,000 years from the Vostok ice core, Antarctica, Nature, 399, 429-436, 1999.

Rehfeld, K., Münch, T., Ho, S. L., and Laepple, T.: Global patterns of declining temperature variability from the Last Glacial Maximum to the Holocene, Nature, 554, 356-359, doi:10.1038/nature25454, 2018.

Risebrobakken, B., Jansen, E., Andersson, C., Mjelde, E., and Hevrøy, K.: A high-resolution study of Holocene paleoclimatic and paleoceanographic changes in the Nordic Seas, Paleoceanography, 18(1), 1017, doi:10.1029/2002PA000764, 2003.

Rodrigues, T., Grimalt, J. O., Abrantes, F. G., Flores, J. A., and Lebreiro, S. M.: Holocene interdependences of changes in sea surface temperature, productivity, and fluvial inputs in the Iberian continental shelf (Tagus mud patch), Geochem. Geophys. Geosyst., 10(7), doi:10.1029/2008GC002367, 2009.

Rodrigues, T., Grimalt, J. O., Abrantes, F., Naughton, F., and Flores, J.-A.: The last glacial–interglacial transition (LGIT) in the western mid-latitudes of the North Atlantic: Abrupt sea surface temperature change and sea level implications, Quaternary Sci. Rev., 29, 1853-1862, doi:10.1016/j.quascirev.2010.04.004, 2010.

Rühlemann, C., Mulitza, S., Müller, P. J., Wefer, G., and Zahn, R.: Warming of the tropical Atlantic Ocean and slowdown of thermohaline circulation during the last deglaciation, Nature, 402, 511-514, 1999.

Sachs, J. P.: Cooling of Northwest Atlantic slope waters during the Holocene, Geophys. Res. Lett., 34, L03609, doi:10.1029/2006GL028495, 2007.

Salzer, M. W., Bunn, A. G., Graham, N. E., and Hughes, M. K.: Five millennia of paleotemperature from tree-rings in the Great Basin, USA, Clim. Dynam., 42, 1517-1526, doi:10.1007/s00382-013-1911-9, 2014.

Saraswat, R., Lea, D. W., Nigam, R., Mackensen, A., and Naik, D. K.: Deglaciation in the tropical Indian Ocean driven by interplay between the regional monsoon and global teleconnections, Earth Planet. Sc. Lett., 375, 166-175, doi:10.1016/j.epsl.2013.05.022, 2013.

Sarnthein, M., van Kreveld, S., Erlenkeuser, H., Grootes, P. M., Kucera, M., Pflaumann, U. and Schulz, M.: Centennial-to-millennial-scale periodicities of Holocene climate and sediment injections off the western Barents shelf, 75°N, Boreas, 32, 447–461, doi:10.1080/03009480310003351, 2003.

Schefuß, E., Schouten, S., and Schneider, R. R.: Climatic controls on central African hydrology during the past 20,000 years, Nature, 437, 1003-1006, doi:10.1038/nature03945, 2005.

Seierstad, I. K., Abbott, P. M., Bigler, M., Blunier, T., Bourne, A. J., Brook, E., Buchardt, S. L., Buizert, C., Clausen, H. B., Cook, E., Dahl-Jensen, D., Davies, S. M., Guillevic, M., Johnsen, S. J., Pedersen, D. S., Popp, T. J., Rasmussen, S. O., Severinghaus, J. P., Svensson, A., and Vinther, B. M.: Consistently dated records from the Greenland GRIP, GISP2 and NGRIP ice cores for the past 104 ka reveal regional millennial-scale δ18O gradients with possible Heinrich event imprint, Quaternary Sci. Rev., 106, 29-46, doi:10.1016/j.quascirev.2014.10.032, 2014.

Seppä, H., and Birks, H. J. B.: July mean temperature and annual precipitation trends during the Holocene in the Fennoscandian tree-line area: pollen-based climate reconstructions, The Holocene, 11(5), 527-539, 2001.

Seppä, H., Hammarlund, D., and Antonsson, K.: Low-frequency and high-frequency changes in temperature and effective humidity during the Holocene in south-central Sweden: implications for atmospheric and oceanic forcings of climate, Clim. Dynam., 25, 285-297, doi:10.1007/s00382-005-0024-5, 2005.

Steig, E. J., Morse, D. L., Waddington, E. D., Stuiver, M., Grootes, P. M., Mayewski, P. A., Twickler, M. S., and Whitlow, S. I.: Wisconsinan and Holocene climate history from an ice core at Taylor Dome, western Ross Embayment, Antarctica, Geogr. Ann., 82 A (2-3), 213-235, 2000.

Steinke, S., Kienast, M., Groeneveld, J., Lin, L.-C., Chen, M.-T., and Rendle-Bühring, R.: Proxy dependence of the temporal pattern of deglacial warming in the tropical South China Sea: toward resolving seasonality, Quaternary Sci. Rev., 27, 688-700, doi:10.1016/j.quascirev.2007.12.003, 2008.

Stenni, B., Masson-Delmotte, V., Selmo, E., Oerter, H., Meyer, H., Röthlisberger, R., Jouzel, J., Cattani, O., Falourd, S., Fischer, H., Hoffmann, G., Iacumin, P., Johnsen, S. J., Minster, B., and Udisti, R.: The deuterium excess records of EPICA Dome C and Dronning Maud Land ice cores (East Antarctica), Quaternary Sci. Rev., 29, 146-159, doi:10.1016/j.quascirev.2009.10.009, 2010.

Stenni, B., Buiron, D., Frezzotti, M., Albani, S., Barbante, C., Bard, E., Barnola, J. M., Baroni, M., Baumgartner, M., Bonazza, M., Capron, E., Castellano, E., Chappellaz, J., Delmonte, B., Falourd, S., Genoni, L., Iacumin, P., Jouzel, J., Kipfstuhl, S., Landais, A., Lemieux-Dudon, B., Maggi, V., Masson-Delmotte, V., Mazzola, C., Minster, B., Montagnat, M., Mulvaney, R., Narcisi, B., Oerter, H., Parrenin, F., Petit, J. R., Ritz, C., Scarchilli, C., Schilt, A., Schüpbach, S., Schwander, J., Selmo, E., Severi, M., Stocker, T. F., and Udisti, R.: Expression of the bipolar see-saw in Antarctic climate records during the last deglaciation, Nat. Geosci., 4, 46-49, doi:10.1038/NGEO1026, 2011.

Stott, L., Poulsen, C., Lund, S., and Thunell, R.: Super ENSO and Global Climate Oscillations at Millennial Time Scales, Science, 297(5579), 222-226, doi:10.1126/science.1071627, 2002.

Stott, L., Cannariato, K., Thunell, R., Haug, G. H., Koutavas, A., and Lund, S.: Decline of surface temperature and salinity in the western tropical Pacific Ocean in the Holocene epoch, Nature, 431, 56-59, doi:10.1038/nature02903, 2004.

Stott, L., Timmermann, A., and Thunell, R.: Southern Hemisphere and Deep-Sea Warming Led Deglacial Atmospheric CO2 Rise and Tropical Warming, Science, 318(5849), 435-438, doi:10.1126/science.1143791, 2007.

Stuiver, M., and Grootes, P. M.: GISP2 Oxygen Isotope Ratios, Quaternary Res., 53, 277-284, doi:10.1006/qres.2000.2127, 2000.

Sun, Y., Oppo, D. W., Xiang, R., Liu, W., and Gao, S.: Last deglaciation in the Okinawa Trough: Subtropical northwest Pacific link to Northern Hemisphere and tropical climate, Paleoceanography, 20, PA4005, doi:10.1029/2004PA001061, 2005.

Taylor, K. C., White, J. W. C., Severinghaus, J. P., Brook, E. J., Mayewski, P. A., Alley, R. B., Steig, E. J., Spencer, M. K., Meyerson, E., Meese, D. A., Lamorey, G. W., Grachev, A., Gow, A. J., and Barnett, B. A.: Abrupt climate change around 22 ka on the Siple Coast of Antarctica, Quaternary Sci. Rev., 23, 7-15, doi:10.1016/j.quascirev.2003.09.004, 2004.

Thompson, L. G., Mosley-Thompson, E., Davis, M. E., Lin, P.-N., Henderson, K. A., Cole-Dai, J., Bolzan, J. F., and Liu, K.-b.: Late Glacial Stage and Holocene Tropical Ice Core Records from Huascarán, Peru, Science, 269(5220), 46-50, doi:10.1126/science.269.5220.46, 1995.

Thornalley, D. J. R., Elderfield, H., and McCave, I. N.: Holocene oscillations in temperature and salinity of the surface subpolar North Atlantic, Nature, 457, 711-714, doi:10.1038/nature07717, 2009.

Tierney, J. E., Russell, J. M., Huang, Y., Damsté, J. S. S., Hopmans, E. C., and Cohen, A. S.: Northern Hemisphere Controls on Tropical Southeast African Climate During the Past 60,000 Years, Science, 322(5899), 252-255, doi:10.1126/science.1160485, 2008.

Tierney, J. E., Pausata, F. S. R., and deMenocal, P.: Deglacial Indian monsoon failure and North Atlantic stadials linked by Indian Ocean surface cooling, Nat. Geosci., 9, 46-50, doi:10.1038/NGEO2603, 2016.

Uemura, R., Masson-Delmotte, V., Jouzel, J., Landais, A., Motoyama, H., and Stenni, B.: Ranges of moisture-source temperature estimated from Antarctic ice cores stable isotope records over glacial–interglacial cycles, Clim. Past, 8, 1109-1125, doi:10.5194/cp-8-1109-2012, 2012.

Veres, D., Bazin, L., Landais, A., Toyé Mahamadou Kele, H., Lemieux-Dudon, B., Parrenin, F., Martinerie, P., Blayo, E., Blunier, T., Capron, E., Chappellaz, J., Rasmussen, S. O., Severi, M., Svensson, A., Vinther, B., and Wolff, E. W.: The Antarctic ice core chronology (AICC2012): an optimized multi-parameter and multi-site dating approach for the last 120 thousand years, Clim. Past, 9, 1733-1748, doi:10.5194/cp-9-1733-2013, 2013.

Vinther, B. M., Buchardt, S. L., Clausen, H. B., Dahl-Jensen, D., Johnsen, S. J., Fisher, D. A., Koerner, R. M., Raynaud, D., Lipenkov, V., Andersen, K. K., Blunier, T., Rasmussen, S. O., Steffensen, J. P., and Svensson, A. M.: Holocene thinning of the Greenland ice sheet, Nature, 461, 385-388, doi:10.1038/nature08355, 2009.

Waelbroeck, C., Duplessy, J.-C., Michel, E., Labeyrie, L., Paillard, D., and Duprat, J.: The timing of the last deglaciation in North Atlantic climate records, Nature, 412, 724-727, 2001.

WAIS Devide Project Members: Onset of deglacial warming in West Antarctica driven by local orbital forcing, Nature, 500, 440-444, doi:10.1038/nature12376, 2013.

Watanabe, O., Kamiyama, K., Motoyama, H., Fujii, Y., Shoji, H., and Satow, K.: The paleoclimate record in the ice core at Dome Fuji station, East Antarctica, Ann. Glaciol., 29, 176-178, 1999.

Watanabe, O., Jouzel, J., Johnsen, S., Parrenin, F., Shoji, H., and Yoshida, N.: Homogeneous climate variability across East Antarctica over the past three glacial cycles, Nature, 422, 509-512, doi:10.1038/nature01525, 2003.

Weijers, J. W. H., Schefuß, E., Schouten, S., and Damsté, J. S. S.: Coupled Thermal and Hydrological Evolution of Tropical Africa over the Last Deglaciation, Science, 315(5819), 1701-1704, doi:10.1126/science.1138131, 2007.

Weldeab, S., Schneider, R. R., Kölling, M., and Wefer, G.: Holocene African droughts relate to eastern equatorial Atlantic cooling, Geology, 33(12), 981-984, doi:10.1130/G21874.1, 2005.

Weldeab, S., Schneider, R. R., and Kölling, M.: Deglacial sea surface temperature and salinity increase in the western tropical Atlantic in synchrony with high latitude climate instabilities, Earth Planet. Sc. Lett., 241, 699-706, doi:10.1016/j.epsl.2005.11.012, 2006.

Weldeab, S., Lea, D. W., Schneider, R. R., and Andersen, N.: 155,000 Years of West African Monsoon and Ocean Thermal Evolution, Science, 316(5829), 1303-1307, doi:10.1126/science.1140461, 2007.

Xu, J., Holbourn, A., Kuhnt, W., Jian, Z., and Kawamura, H.: Changes in the thermocline structure of the Indonesian outflow during Terminations I and II, Earth Planet. Sc. Lett., 273, 152-162, doi:10.1016/j.epsl.2008.06.029, 2008.

Zhao, M., Beveridge, N. A. S., Shackleton, N. J., Sarnthein, M., and Eglinton, G.: Molecular stratigraphy of cores off northwest Africa: Sea surface temperature history over the last 80 ka, Paleoceanography, 10(3), 661-675, 1995.

Zhao, M., Huang, C.-Y., Wang, C.-C., and Wei, G.: A millennial-scale UK′37 sea-surface temperature record from the South China Sea (8°N) over the last 150 kyr: Monsoon and sea-level influence, Palaeogeogr. Palaeocl., 236, 39-55, doi:10.1016/j.palaeo.2005.11.033, 2006.

Ziegler, M., Nürnberg, D., Karas, C., Tiedemann, R., and Lourens, L. J.: Persistent summer expansion of the Atlantic Warm Pool during glacial abrupt cold events, Nat. Geosci., 1, 601-605, doi:10.1038/ngeo277, 2008.